

Identification and transcriptomic profiling of salinity stress response genes in colored wheat mutant

Min Jeong Hong¹, Chan Seop Ko¹, Jin-Baek Kim¹, Dae Yeon Kim^{Corresp. 2}

¹ Advanced Radiation Technology Institute, Korea Atomic Energy Research institute, Jeongeup, Jeollabuk-do, Korea

² Plant Resources, Kongju National University, Yesan-eup, Chungnam, South Korea

Corresponding Author: Dae Yeon Kim
Email address: dykim@kongju.ac.kr

Background. Salinity stress is a major abiotic stress that prevents normal plant growth and development, ultimately reducing crop productivity. This study investigated the effects of salinity stress on two wheat lines: PL1 (wild type) and PL6 (mutant line generated through gamma irradiation of PL1).

Results. Salinity stress negatively impacted germination and plant growth in both lines, but PL6 exhibited higher tolerance. PL6 showed lower Na⁺ accumulation and higher K⁺ levels, indicating better ion homeostasis. Genome-wide transcriptomic analysis revealed distinct gene expression patterns between PL1 and PL6 under salt stress, resulting in notable phenotypic differences. Gene ontology analysis revealed positive correlations between salt stress and defense response, glutathione metabolism, peroxidase activity, and reactive oxygen species metabolic processes, highlighting the importance of antioxidant activities in salt tolerance. Additionally, hormone-related genes, transcription factors, and protein kinases showed differential expression, suggesting their roles in the differential salt stress response. Enrichment of pathways related to flavonoid biosynthesis and secondary metabolite biosynthesis in PL6 may contribute to its enhanced antioxidant activities. Furthermore, differentially expressed genes associated with the circadian clock system, cytoskeleton organization, and cell wall organization shed light on the plant's response to salt stress.

Conclusions. Understanding these mechanisms is crucial for developing stress-tolerant crop varieties, improving agricultural practices, and breeding salt-resistant crops to enhance global food production and address food security challenges.

1 **Identification and Transcriptomic Profiling of Salinity Stress**
2 **Response Genes in Colored Wheat Mutant**

3

4 Min Jeong Hong¹, Chan Seop Ko¹, Jin-Baek Kim¹

5 ¹ Advanced Radiation Technology Institute, Korea Atomic Energy Research Institute, 29

6 Geungu, Jeongeup 56212, Korea

7

8 Corresponding Author:

9 Dae Yeon Kim²

10 ² Department of Plant Resources, Kongju National University, 54 Daehak-ro Yesan-eup

11 Chungnam 322439, Korea

12 Email Address dykim@kongju.ac.kr

13

14 **Abstract**

15 **Background.** Salinity stress is a major abiotic stress that prevents normal plant growth and
16 development, ultimately reducing crop productivity. This study investigated the effects of salinity
17 stress on two wheat lines: PL1 (wild type) and PL6 (mutant line generated through gamma
18 irradiation of PL1).

19 **Results.** Salinity stress negatively impacted germination and plant growth in both lines, but PL6
20 exhibited higher tolerance. PL6 showed lower Na⁺ accumulation and higher K⁺ levels, indicating
21 better ion homeostasis. Genome-wide transcriptomic analysis revealed distinct gene expression
22 patterns between PL1 and PL6 under salt stress, resulting in notable phenotypic differences. Gene
23 ontology analysis revealed positive correlations between salt stress and defense response,
24 glutathione metabolism, peroxidase activity, and reactive oxygen species metabolic processes,
25 highlighting the importance of antioxidant activities in salt tolerance. Additionally, hormone-
26 related genes, transcription factors, and protein kinases showed differential expression, suggesting
27 their roles in the differential salt stress response. Enrichment of pathways related to flavonoid
28 biosynthesis and secondary metabolite biosynthesis in PL6 may contribute to its enhanced
29 antioxidant activities. Furthermore, differentially expressed genes associated with the circadian
30 clock system, cytoskeleton organization, and cell wall organization shed light on the plant's
31 response to salt stress.

32 **Conclusions.** Understanding these mechanisms is crucial for developing stress-tolerant crop
33 varieties, improving agricultural practices, and breeding salt-resistant crops to enhance global food
34 production and address food security challenges.

35

36 **Introduction**

37 Climate change and global warming cause various environmental stresses, such as temperature
38 fluctuations, droughts, floods, and increased salinity, which have detrimental effects on crop
39 productivity (Kissoudis *et al.*, 2014). Among these stresses, salinity stress is a significant abiotic
40 factor that hampers plant growth and development, leading to decreased agricultural productivity
41 (Amirbakhtiar *et al.*, 2019; Al-Ashkar *et al.*, 2019). The impact of salinity is extensive, with >20%
42 of irrigated land worldwide being affected. Furthermore, it is projected that up to 50% of arable
43 land will be lost by 2050 owing to salinization caused by both human activities and ongoing
44 climate change (Asif *et al.*, 2018; Kumar & Sharma, 2020; Chele *et al.*, 2021).

45 Wheat is a crucial crop cultivated globally, contributing to 30% of global grain production and
46 providing approximately 20% of the calories consumed by humans (Shiferaw *et al.*, 2013;
47 Seleiman *et al.*, 2022). Soil salinity poses a critical issue, resulting in yield losses of up to 60% in
48 wheat production (El-Hendawy *et al.*, 2017). Salinity stress disrupts plant growth by increasing
49 Na⁺ ion assimilation and reducing the Na⁺/K⁺ ratio, leading to osmotic stress and ion toxicity,
50 consequently affecting normal plant development (EL Sabagh *et al.*, 2021). Additionally, under
51 salinity stress, oxidative stress can impair plant growth through reduced photosynthetic capacity,
52 oxidative damage caused by an imbalance in reactive oxygen species (ROS) production, and

53 decreased antioxidant activity, ultimately leading to reduced crop yield (*Hasanuzzaman et al.*,
54 2014; *Sadak, 2019; Omrani et al., 2022*).

55 Numerous studies have focused on breeding new salt-tolerant crop varieties using molecular and
56 biology-based technologies (*Huang et al., 2008; Ismail & Horie, 2017; Saade et al., 2020; Hussain*
57 *et al., 2021*). Regulating excessive Na⁺ accumulation in plants is a vital strategy for enhancing salt
58 resistance (*Tester & Davenport, 2003; Møller & Tester, 2007; Møller et al., 2009*). The high-
59 affinity K⁺ transporter (HKT) gene family plays a crucial role in maintaining Na⁺ and K⁺ balance
60 in plant growth, development, abiotic stress responses, and salt tolerance (*Horie et al., 2009; Li et*
61 *al., 2019; Riedelsberger et al., 2021*). Initially identified in wheat (*Schachtman & Schroeder,*
62 *1994*), HKT genes have been found to reduce Na⁺ accumulation in higher plants, such as
63 *Arabidopsis*, rice, and wheat (*Riedelsberger et al., 2021*). Additionally, the salt overly sensitive
64 (SOS) gene family is involved in regulating ion homeostasis and Na⁺ exclusion at the cellular
65 level, affecting plant salinity tolerance (*Yang et al., 2009*).

66 Various screening parameters are used to select salt-tolerant crops, including germination rate (*El-*
67 *Hendawy et al., 2019; Choudhary et al., 2021*), plant growth (*Sayed, 1985*), chlorophyll content
68 (*Tsai et al., 2019*), and K⁺/Na⁺ ratio (*Assaha et al., 2017; Singh & Sarkar, 2014*). Particularly, the
69 germination and growth rates during the early stages of plant development have proven useful for
70 screening salt-tolerant crops (*Choudhary et al., 2021*). In *Brassica napus*, root and shoot lengths
71 act as early indicators for evaluating salt tolerance (*Long et al., 2015*). In rice, salt-tolerant cultivars
72 have higher chlorophyll content and Na⁺/K⁺ ratios under salt stress conditions than salt-susceptible
73 cultivars (*Singh & Sarkar, 2014*).

74 Despite ongoing research on gene regulation under salt stress, limited progress has been made in
75 establishing appropriate screening methods using genetic resources, understanding mechanisms
76 underlying osmotic stress/tissue resistance, and identifying salt-tolerant crops (*Genc et al., 2019*).
77 Furthermore, as elite germplasm may lack genes that confer salt resistance, genetic engineering
78 involving the artificial insertion of specific genes may be required to develop new crop varieties
79 (*Colmer et al., 2006; Shavrukov et al., 2009; Munns et al., 2012; Deinlein et al., 2014*).

80 Genetic diversity is crucial for developing new and improved crop varieties with desirable traits.
81 However, breeders often focus on improving traits by selecting offspring with the best attributes,
82 leading to a decrease in genetic diversity when some plants become vulnerable to environmental
83 stresses. Mutation breeding is a widely used method for enhancing genetic diversity and improving
84 crop traits. Gamma rays, being physical mutagens, are commonly used for plant mutation breeding
85 and have been instrumental in developing >50% of the 3,401 new varieties included in the
86 FAO/IAEA Mutant Variety Database (<https://nucleus.iaea.org/sites/mvd/SitePages/Home.aspx>).
87 In light of these findings, the construction of a mutant pool using gamma rays offers an opportunity
88 to develop salt-resistant wheat by securing genetic diversity. Therefore, this study selected the salt-
89 resistant colored wheat mutant PL6 (developed via gamma ray mutagenesis) and investigated its
90 salt resistance mechanism induced by gamma ray mutation through transcriptome analysis of PL6

91 and wild-type (PL1) wheat. Breeding salt-tolerant crops is challenging owing to the complexity of
92 polygenic traits resulting from genetic and physiological diversity (*Genc et al., 2019; Hanin et al.,*
93 *2016*). The findings of this study provide valuable insights for breeding salt-tolerant wheat and
94 offer various interpretations of salt tolerance.

95

96 **Materials & methods**

97 **Plant materials**

98 In this study, we incorporated the hexaploid wheat inbred line K4191, which possesses deep purple
99 grain color. K4191 (hereafter termed PL1) was derived from the F_{4:8} generation resulting from the
100 cross between ‘Woori-mil’ (obtained from the National Agrobiodiversity Center, RDA, Korea;
101 accession no. IT172221) and ‘D-7’ (an inbred line developed by Korea University;
102 Fleming4/3/PIO2580//T831032/Hamlet) (*Hong et al., 2019*). To induce genetic variation and
103 diversify the population of colored wheat, colored wheat seeds were irradiated with 200 Gy gamma
104 rays at a dose rate of 25 Gy/h using a ⁶⁰Co gamma irradiator (150 TBq of capacity; Noridon,
105 Ottawa, ON, Canada) at the Korea Atomic Energy Research Institute. Subsequently, the irradiated
106 seeds were planted at the radiation breeding research farm. The resulting mutants were
107 continuously cultivated up to the M₆ generation and carefully selected based on excellent
108 agricultural traits, including flowering time, plant height, yield, and grain color. In total, 50 mutant
109 lines displaying stable phenotypes for at least two generations were chosen for further salt-
110 tolerance screening. For the preliminary screening of the selected mutant lines, 100 seeds from
111 each line were placed in a phytohealth chamber (SPL Life Sciences, Pocheon, Korea) with two
112 layers of germination paper, and a total volume of 200 mL of the solution containing 150 mM
113 NaCl was applied to the seeds at a temperature of 22°C. After 4 days, the germination rate and
114 shoot and root lengths were recorded, and salinity-resistant lines were identified. Among the tested
115 mutants, one specific mutant, named PL6, demonstrated exceptional salt tolerance, exhibiting a
116 high germination rate and favorable growth characteristics. Therefore, PL6 was chosen for further
117 detailed analysis in the context of salt tolerance, and the hexaploid wheat inbred line PL1 was used
118 as the control line.

119 **Salt stress treatment**

120 The PL1 (control line, K4191) and PL6 (mutant line) seeds were surface-sterilized with 70%
121 ethanol for 1 min and then washed with sterile distilled water. Subsequently, the seeds were placed
122 on moist filter papers in a Petri dish (SPL Life Sciences) until the first leaf of the seedlings
123 appeared. Next, the uniformly germinated seeds were transferred to Incu Tissue culture vessels
124 (SPL Life Sciences) filled with half-strength Hoagland’s culture solution. The solutions were
125 replaced daily. The seedlings were grown for 7 days in a well-controlled chamber at 22°C and
126 60% humidity, with a photoperiod regime of 16/8 h day/night at 200–300 μmol m⁻²s⁻¹ light. After
127 7 days of transplanting, the seedlings were subjected to a salt stress treatment of a total volume of
128 200 mL of the solution containing 150 mM NaCl. Following treatment with 150 mM NaCl, the
129 wheat leaves were collected at 3, 24, and 48 h. Both control and salt-stressed seedlings were
130 collected individually. The samples were immediately frozen in liquid nitrogen and stored at
131 –80°C until use in further experiments.

132 **Measurement of leaf Na⁺ and K⁺ contents**

133 The wheat leaves were collected separately and immediately frozen in liquid nitrogen.
134 Subsequently, the samples were freeze-dried for 3 days in a Freeze Dry System (IlshinBioBase,
135 Dongducheonsi, Gyeonggi, Korea). The freeze-dried samples were then finely ground into a powder
136 using a mortar and pestle. For further analysis, 50 mg of the freeze-dried samples was weighed
137 using an analytical balance and boiled for 2 h at 200°C in 3 mL of HNO₃ (70%, v/v) for digestion.
138 After digestion, the extracted samples were diluted with 5% HNO₃ and filtered through a
139 hydrophilic polytetrafluoroethylene syringe filter (0.45-μm pore size, 25-mm diameter). The shoot
140 Na⁺ and K⁺ contents were measured using inductively coupled plasma atomic emission
141 spectroscopy (ICP-AES, 720 series; Agilent, Santa Clara, CA, USA) and quantitatively analyzed
142 using a VistaChip II CCD detector (Agilent).

143 **Measurement of chlorophyll content**

144 To determine the chlorophyll content, wheat seedling samples were extracted with 100% methanol
145 at 4°C. The sample extracts were then subjected to centrifugation at 12,000 ×g for 10 min, and the
146 supernatant was used for chlorophyll content analysis. The total chlorophyll, chlorophyll a, and
147 chlorophyll b concentrations were determined by measuring the absorbance at 644.8 and 661.6 nm
148 using a UV-VIS spectrophotometer (*Lichtenthaler, 1987*). The chlorophyll concentration was
149 calculated using the following equations:

$$150 \quad C_a = 11.24 \times A_{661.6} - 2.04 \times A_{644.8}$$

$$151 \quad C_b = 20.13 \times A_{644.8} - 4.19 \times A_{661.6}$$

$$152 \quad C_{\text{total}} = 7.05 \times A_{661.6} + 18.09 \times A_{644.8}$$

153 where C_a, C_b, and C_{total} denote the concentrations of chlorophyll a, chlorophyll b, and total
154 chlorophyll, respectively.

155 **RNA sequencing and gene expression analyses**

156 Total RNA was extracted from the wheat leaves of both PL1 and PL6 at each timepoint (0, 3, 24,
157 and 48 h) using TRIzol (Invitrogen, Carlsbad, CA, USA) following the manufacturer's
158 instructions. Two independent biological replicates were performed for each timepoint and line to
159 ensure the reliability and reproducibility of the RNA-seq data. Additionally, the extracted RNA
160 samples were treated with DNase I to remove any potential genomic DNA contamination. The
161 RNA quality was assessed using an Agilent 2100 bioanalyzer (Agilent Technologies, Amstelveen,
162 The Netherlands), and RNA quantification was performed using an ND-2000 Spectrophotometer
163 (Thermo Inc.; Wilmington, DE, USA). For constructing the RNA-seq paired-end libraries, 10 μg
164 of total RNA extracted from the samples was used with the TruSeq RNA Sample Preparation Kit
165 (Catalog #RS-122-2001; Illumina, San Diego, CA, USA). The mRNA was isolated using a
166 Poly(A) RNA Selection Kit (LEXOGEN, Inc.; Vienna, Austria) and reverse-transcribed into
167 cDNA following the manufacturer's instructions. The libraries were assessed using the Agilent
168 2100 bioanalyzer, and the mean fragment size was evaluated using a DNA High Sensitivity Kit
169 (Agilent, Santa Clara, CA, USA). High-throughput sequencing was conducted using the HiSeq
170 2000 platform (Illumina). Before alignment, adaptor sequences were removed, and sequence

171 quality was evaluated using the Bbduk tool (minimum length > 20 and Q > 20;
172 <https://jgi.doe.gov/data-and-tools/software-tools/bbtools/bb-tools-user-guide/bbduk-guide/>). The
173 reads were aligned to the wheat genome sequence provided by the International Wheat Genome
174 Sequencing Consortium (IWGSC) wheat reference sequence (IWGSC Reference Sequence v1.0;
175 https://urgi.versailles.inra.fr/download/iwgsc/IWGSC_RefSeq_Annotations/v1.0/) using the
176 HISAT2 alignment program with default parameters (Kim *et al.*, 2015). Reads mapped to the exons
177 of each gene were enumerated using the HTSeq v0.6.1 high-throughput sequencing framework
178 (Anders *et al.*, 2015). Subsequently, the differentially expressed genes (DEGs) under salt stress
179 and control conditions were identified using the EdgeR package (Robinson *et al.*, 2010).
180 Upregulated and downregulated genes with a p-value of <0.05, false discovery rate (FDR) of
181 <0.05, and an absolute fold change value of >2 were used for downstream functional analysis. The
182 log₂-transformed transcript per million values were calculated using TPMCalculator (Vera
183 Alvarez *et al.*, 2019), and heatmaps of DEGs under control and stress conditions were generated.
184 Local BlastX was used with peptide sequences of the Poaceae family retrieved from the National
185 Center for Biotechnology Information (NCBI) database using an e-value threshold of 1×10^{-5} to
186 annotate the DEGs. For gene expression analysis, total RNA was used to synthesize first-strand
187 cDNA using the Power cDNA Synthesis Kit (iNtRON Biotechnology, Gyeonggi-do, Korea).
188 Reverse transcription-quantitative polymerase chain reaction (RT-qPCR) was performed in a total
189 volume of 20 μ L containing 1 μ L of cDNA template, 0.2 μ M primers, and 10 μ L of TB Green
190 Premix Ex Taq II (Takara, Kusatsu, Shiga, Japan). RT-qPCR was conducted using a CFX96TM
191 Real-time PCR system (Bio-Rad, Hercules, CA, USA) with the following program: 95°C for 5
192 min, followed by 40 cycles at 95°C for 10 s and 65°C for 30 s. Actin (AB181991) was used as an
193 internal control. The primers used in this experiment are listed in Table S1.

194 **Functional analysis of DEGs**

195 All expressed genes under both control and stress conditions were subjected to Gene Set
196 Enrichment Analysis (GSEA) using the GSEA software (Subramanian *et al.*, 2005). The gene
197 matrix transposed file format (.GMT) of wheat was downloaded from g:Profiler
198 (<https://biit.cs.ut.ee/gprofiler/gost>), a web server for functional enrichment analysis and gene list
199 conversion (Raudvere *et al.*, 2019). The enrichment score of each gene set was calculated using
200 the full ranking, and the normalized enrichment score (NES) was determined for each gene set.
201 The GSEA results, including rank, expression, and class files, were visualized as a network using
202 Enrichment Map (Merico *et al.*, 2010). For Kyoto Encyclopedia of Genes and Genome (KEGG)
203 pathway enrichment analysis, the KEGG Orthology Database in KOBAS-i was used to predict the
204 putative pathways of DEGs (Bu *et al.*, 2021). The plant transcription factor data were obtained
205 from the Plant Transcription Factor Database (PlantTFDB) (Tian *et al.*, 2020). Protein Basic Local
206 Alignment Search Tool (BLASTP) was used on the peptide sequences of the DEGs, based on the
207 local transcription factor database obtained from PlantTFDB, with an E-value threshold of 1×10^{-1}
208 and sequence identity of >80%. Mev software ([http://sourceforge.net/projects/mev-tm4/files/mev-](http://sourceforge.net/projects/mev-tm4/files/mev-tm4/)
209 [tm4/](http://sourceforge.net/projects/mev-tm4/files/mev-tm4/)) was used for k-means clustering of DEGs identified from the GSEA, KEGG pathway, and
210 transcription factor analyses. The results of the GSEA and KEGG pathway analysis were generated
211 using an R script and the ggplot2 R package. Additionally, MapMan (Sreenivasulu *et al.*, 2008)
212 was used to identify the pathways of stage-specific genes.

213 Enzyme activities assays

214 The crude enzyme was extracted from 100 mg of wheat leaves using a protein extraction buffer
215 containing 50 mM potassium phosphate buffer (pH 7.5). The activities of catalase (CAT),
216 peroxidase (POD), and superoxide dismutase (SOD) and total antioxidant activity (TAC) were
217 measured using commercially available assay kits. Specifically, CAT activity was determined
218 using a catalase microplate assay kit (kit number: MBS8243260; MyBiosource, Inc., San Diego,
219 CA, USA), POD activity was measured using a POD assay kit (kit number: KTB1150; Abbkine,
220 Inc., Wuhan, China), and SOD activity was estimated using a total SOD activity assay kit (WST-
221 1 method) (kit number: MBS2540402; MyBiosource, Inc., San Diego, CA, USA). TAC was
222 assessed using a TAC assay kit (kit number: MAK187; Sigma-Aldrich, St. Louis, MO, USA). The
223 preparation of the reaction mixture and the calculations for each measurement were performed as
224 described in the respective protocol books provided with each assay kit.

225

226 Results

227 Characteristics of the salt-tolerant colored wheat mutant induced via gamma irradiation

228 In this study, the hexaploid wheat inbred line PL1, which possessed a deep purple grain color, was
229 used as the control line for mutation breeding. Briefly, 1500 M_0 seeds were exposed to irradiation,
230 and the resulting seeds were sown to generate the M_1 generation. Among these seeds, 287
231 phenotypically distinctive lines were carefully selected with one spike per plant, and mutation
232 breeding spanning from M_0 to M_4 was performed as thoroughly described in a previous study
233 (Hong *et al.*, 2019). For the current study, the M_6 generations of PL1 and PL6 were used.
234 Throughout the mutation breeding process, detailed records of agricultural traits, including the
235 flowering time, plant height, and yield, were meticulously collected for the mutant lines. These
236 data allowed for a comprehensive assessment of the phenotypic characteristics of the lines.
237 Evidence supporting the stable phenotype of the mutant lines is provided in Fig. S1, which also
238 presents the field performance of PL1 and PL6. Additionally, the difference in grain color between
239 the colored wheat lines used in this study and common wheat lines cultivated in Korea is illustrated
240 in Fig. S2. Through preliminary salt-tolerance screening, PL6 was selected as the gamma ray-
241 derived mutant line that exhibited favorable salt-tolerance characteristics (Fig.S3). To assess the
242 growth response of the control line (PL1) and PL6 under varying salt concentrations, the seeds
243 were treated with NaCl solutions of 50, 100, 150, 200, 250, 300, and 500 mM, along with distilled
244 water as the control (Choudhary *et al.*, 2021). Overall, high salt concentrations negatively affected
245 seed germination and seedling growth (Figs. 1A and 1B). The germination percentage and seedling
246 growth were reduced with increasing salt concentration in both PL1 and PL6 (Table S2). However,
247 PL6 demonstrated higher germination percentages, particularly at the maximum NaCl
248 concentration, exceeding those of PL1. Remarkably, a maximum increase of 20% in germination
249 was observed for PL6 following treatment with 250 mM NaCl. Moreover, PL6 consistently
250 outperformed PL1 in terms of seedling growth under all salt treatment conditions, as evidenced by
251 its longer shoot and root lengths (Figs. 1C and 1D). The comprehensive data strongly indicates
252 that the gamma ray-derived mutant PL6 exhibits higher resistance to salt stress than PL1.

253 **Assessment of Na⁺, K⁺, and chlorophyll contents under salt stress conditions**

254 To evaluate the changes in Na⁺ and K⁺ ion contents in response to salt stress, wheat leaves were
255 collected at 3, 24, and 48 h after salt treatment. Prior to treatment, PL6 had a higher Na⁺ ion content
256 than PL1 (Fig. 2A). However, with increasing time of exposure to salt stress, the Na⁺ ion content
257 markedly increased in both PL1 and PL6. Notably, the rate of increase in Na⁺ ion content was
258 lower in PL6 than in PL1. Conversely, the K⁺ ion content steadily decreased with salt treatment in
259 both PL1 and PL6 (Fig. 2B). To further analyze the ion contents, we calculated the relative ratios
260 of K⁺ and Na⁺ ions in PL1 and PL6, considering their respective contents under control conditions
261 (Figs. 2C and 2D). In PL1, the Na⁺ ion content increased significantly by 47 times from the
262 baseline (0 h) to 48 h following salt treatment. In contrast, PL6 exhibited a milder increase in Na⁺
263 ion content, approximately 20 times higher at 48 h after salt stress. Consequently, the relative Na⁺
264 content was more profoundly affected by salt stress in PL1 than in PL6. Interestingly, the
265 chlorophyll concentrations of both PL1 and PL6 remained relatively stable under salt stress (Fig.
266 2E), indicating that they were not significantly affected by the imposed salinity conditions.

267 **DEGs during salt stress**

268 After treatment with 150 mM NaCl, leaves were harvested from PL1 and PL6 at 3, 24, and 48 h
269 and subjected to RNA sequencing. Following quality evaluation and trimming, an average of 38.1
270 million trimmed reads and over 22.1 billion bases were generated from each sample under both
271 control and salt stress conditions. The average percentage of Q20 and Q30 bases was found to be
272 98.4% and 95.5%, respectively, indicating high sequencing quality. Moreover, >96% of the
273 sequenced data exhibited an average mapping rate of 96.16%, successfully aligning to the IWGSC
274 wheat reference sequence (Table S3). During data analysis, a total of 4,017 DEGs were identified
275 with a p-value of <0.05, FDR of <0.05, and absolute fold change value of >2 (Fig. 3A and Table
276 S4). Specifically, in PL1, 872, 1,588, and 1,080 DEGs were detected at 3, 24, and 48 h after salt
277 treatment, respectively, compared with those detected without treatment (Fig. 3B). For PL6, the
278 numbers of DEGs were 566, 1,248, and 1,810 at 3, 24, and 48 h after salt treatment, respectively
279 (Fig. 3C). These results highlight the dynamic gene expression changes in PL1 and PL6 under salt
280 stress at different timepoints, contributing to a better understanding of the underlying molecular
281 responses to salt stress in these wheat lines.

282 **Functional analysis of the DEGs during salt stress**

283 To identify the differences in gene ontology (GO) term enrichment between PL1 and PL6 during
284 salt stress, all the DEGs of PL1 and PL6 at different timepoints were analyzed using GSEA with
285 a default parameter. Overall, 33 GO terms were identified for each treatment condition (Fig. 3D
286 and Table S5). Notably, several gene sets, including defense response (GO: 0006952), glutathione
287 metabolic process (GO: 0006749), peroxidase activity (GO: 0004601), ROS metabolic process
288 (GO: 0072593), response to biotic stimulus (GO: 0009607), and response to stress (GO: 0006950),
289 were positively correlated with salt stress and PL6, exhibiting a positive NES (Fig. 3D). To
290 visualize the results, all the gene sets from the GSEA were organized into four networks using
291 Enrichment Map (*Merico et al., 2010*) (Figs. 4A–4E). The expression patterns of each network in
292 Figs. 4A–4E for PL1 and PL6 were clustered by expressed patterns (Figs. 4F–4J, respectively).
293 The K-means clustering algorithm in the Mev software was used to identify the clusters of DEGs
294 in each GO term under control and salt stress conditions based on their expression patterns. Most

295 of the expression patterns from the identified clusters did not differ between the control and salt
296 stress conditions. Three clusters that demonstrated different expression patterns for PL1 and PL6,
297 especially those upregulated in PL6, were selected and marked in red boxes in Figs. 4F, 4G, and
298 4I, and a heatmap of the genes from these clusters was generated (Fig. 4K). Plant hormone-related
299 genes (*TRAESCS1B02G145800* and *TRAESCS1B02G138100*), ROS-related genes
300 (*TRAESCS1B02G059100*, *TRAESCS1B02G095800*, *TRAESCS1B02G096200*,
301 *TRAESCS1B02G096900*, and *TRAESCS1B02G115900*), and stress-response genes
302 (*TRAESCS5D02G492900*, *TRAESCS1A02G009900*, *TRAESCS1B02G023000*, and
303 *TRAESCS2A02G037400*) were highly expressed in PL6 under salt stress conditions. Furthermore,
304 six genes related to chromatin remodeling (*TRAESCS1B02G048900*, *TRAESCS1B02G049100*,
305 *TRAESCS1D02G286700*, *TRAESCS1B02G149000*, and *TRAESCS7D02G246600*) showed high
306 expression patterns in PL6 under salt stress conditions (Table 1). A high number of transcriptomes
307 of MADS-box transcription factors (*TRAESCS4A02G002600*, and *TRAESCS6D02G293200*) were
308 also detected in PL6 under salt stress. An auxin-responsive protein (*TRAESCS1B02G138100*) and
309 probable histone H2A variant 3 (*TRAESCS7D02G246600*) were also found in cluster 4 (Table 1).

310 In the case of the differences in the KEGG pathways between PL1 and PL6 under salt stress
311 conditions, the rich factor of “Biosynthesis of secondary metabolites” in PL6 after 3 h of salt stress
312 was ~0.05, increasing to ~0.2 after 48 h of salt stress (Fig. 5). Likewise, the rich factors of
313 “Flavonoid biosynthesis” were 0.17 and 0.23, after 24 and 48 h of salt stress, respectively. This
314 was only observed in PL6 during salt stress conditions (Fig. 5 and Table S6).

315 In addition to GO and KEGG analysis, the role of DEGs as transcription factors was investigated.
316 DEGs at different timepoints under salt stress in PL1 and PL6 were identified using PlantTFDB
317 (<http://planttfdb.gao-lab.org>). In total, 255 genes were identified with an e-value threshold of $1 \times$
318 10^{-1} and a sequence identity of >80% and further selected to compare the expression patterns
319 between PL1 and PL6 under salt stress conditions. The most abundant type of transcription factor
320 was the ethylene-response factor (ERF) protein family, followed by the basic helix-loop-helix
321 (bHLH) protein family; heat shock transcription factor protein family; myeloblastosis (MYB)-
322 related protein family; and Nam, ATAF, and CUC (NAC) protein family (Fig. 6A). Moreover, 255
323 putative transcription factors were grouped by expression pattern into six clusters and an
324 unclassified group (Fig. 6B). Overall, 72, 44, and 35 DEGs were annotated by the ERF, bHLH,
325 and MYB (related) protein families, respectively. These three transcription factors accounted for
326 59% of the total number of transcription factors. The expression patterns of DEGs in clusters 2
327 and 6 (marked with red boxes in Fig. 6B) were selected and expressed in heatmaps (Fig. 6C) to
328 display differences in the expression patterns of DEGs between PL1 and PL6 under salt stress
329 conditions (Table S7). Notably, PL6 exhibited higher expression of specific transcription factors
330 under salt stress conditions than PL1, as displayed in the heatmap (Fig. 6C).

331 Lastly, 22 protein kinase genes were identified with significant expression patterns at different
332 timepoints, including two calcineurin B-like (CBL)-interacting protein kinases and one mitogen-
333 activated protein kinase (MAPK) with more than two-fold changes in PL6 under salt stress (Table
334 2). Additionally, 70 differentially expressed salt stress-responsive genes involved in regulating the
335 circadian clock system, cytoskeleton organization, and cell wall organization were identified using
336 MapMan, with 15 of them showing more than a two-fold change in PL6 (Table 3).

337 Enzyme activities assays

338 To investigate the differences in enzyme activities between PL1 and PL6 under salt stress
339 conditions, we measured CAT, POD, and SOD activities and TAC (Fig. 7). Upon subjecting both
340 wheat lines to salt stress, we observed distinct patterns in enzyme activities. In PL6, CAT and POD
341 activities significantly increased after 24 and 48 h of exposure to salt stress (Fig. 7A and B).
342 Conversely, in PL1, SOD activity slightly decreased after 24 and 48 h exposure to salt stress (Fig.
343 7C). Furthermore, the TAC in PL1 was not significantly changed by salt stress (Fig. 7D).
344 Conversely, in PL6, the TAC notably increased after 24 and 48 h of exposure to salt stress. This
345 increase in TAC suggests that PL6 has a higher capacity to counteract oxidative stress and maintain
346 cellular redox balance than PL1, contributing to its enhanced salinity tolerance.

347 Validation of the DEG results using reverse transcription-quantitative polymerase chain 348 reaction

349 Supporting the DEG results, 12 genes from the three aforementioned clusters from PL1 and PL6
350 were selected for RT-qPCR (Fig. 8). All the selected genes were more highly expressed in PL6
351 than in PL1. *peroxidase 2* (TRAESCS1B02G095800), *nitrate transporter*
352 (TRAESCS1B02G038700), *auxin-responsive protein* (TRAESCS1B02G138100), and *replication*
353 *protein A* (TRAESCS1B02G102200) transcripts in PL6 were highly expressed at 48 h following
354 salt treatment (Fig. 8A). *Nuclear transport factor 2- like protein* (TRAESCS2A02G046200),
355 *histone H2A* (TRAESCS1B02G048900), *integral membrane protein* (TRAESCS1B02G071800),
356 and *histone H2A variant 3* (TRAESCS7D02G246600) transcripts in PL6 continuously decreased
357 at 24 h and peaked at 48 h following salt treatment (Fig. 8B). *Argonaute 1C-like isoform X2*
358 (TRAESCS6B02G466700), *MADS-box* (TRAESCS6B02G017900), and *aspartokinase 1*
359 (TRAESCS5D02G537600) transcripts in PL6 peaked at 3 h, and all gradually decreased, except
360 for *ribosome biogenesis protein NOP53* (TRAESCS1B02G105100) (Fig. 8C). These results are
361 consistent with those of RNA sequencing (RNA-seq).

362

363 Discussion

364 This study revealed that salinity stress had negative effects on germination and plant growth during
365 the developmental process. Na⁺ is considered a nonessential element in plants (Nieves-Cordones
366 *et al.*, 2016); however, excessive accumulation of Na⁺ can have detrimental effects on plants,
367 including disrupting cellular homeostasis, inducing oxidative stress, and suppressing growth
368 (Munns & Tester, 2008; Craig Plett, 2010). The observed differences in germination between PL1
369 and PL6 under salt stress conditions were noteworthy. PL6 demonstrated a higher germination rate
370 than PL1 at all salt treatment concentrations (Figs. 1A and 1B and Table S2). Additionally, PL1
371 exhibited higher sensitivity to salt stress during seedling growth, resulting in considerably shorter
372 shoot and root lengths compared with PL6 (Figs. 1C and 1D). These findings are consistent with
373 the variations in K⁺ and Na⁺ contents between PL1 and PL6 (Fig. 2). Furthermore, the additional
374 accumulation ratio of Na⁺ increased drastically in PL1 with the duration of the salt treatment, while
375 no significant change was observed in PL6 (Fig. 2D). Previous research on different rice genotypes
376 demonstrated varying germination rates and nutrient survival under salt stress, which was
377 associated with differences in ion concentration and homeostasis (Craig Plett, 2010). Similarly,

378 reduction of Na⁺ accumulation and maintenance of K⁺ accumulation in the shoots have been shown
379 to play an important role in salinity tolerance in barley and maize (*Tester & Davenport, 2003*;
380 *Chen et al., 2007*).

381 Genome-wide transcriptomic analysis has emerged as a powerful tool to investigate stress-tolerant
382 genes, gene families, and related mechanisms in plants (*Peng et al., 2014*; *Li et al., 2016*). In this
383 study, we observed a significant difference in the salinity response between PL1 and PL6 and
384 identified distinct expression patterns of DEGs between the two lines. Although a higher number
385 of DEGs was found in PL6 compared with PL1, it is important to note that the majority of these
386 DEGs exhibited similar expression patterns in both PL1 and PL6 under salt stress conditions. This
387 could be because PL6 was generated through a mutation of PL1 via gamma irradiation, leading to
388 the sharing of numerous genomes between them. Nonetheless, despite the similar expression
389 patterns, clear phenotypic differences were observed, including variations in germination rate,
390 shoot and root growth, and ion concentrations (Na⁺ and K⁺). Thus, our genome-wide
391 transcriptional analysis allowed us to identify the DEGs responsible for the differential responses
392 of PL1 and PL6 under salt stress conditions.

393 Salt stress not only induces osmotic stress but also leads to ionic imbalance, resulting in ion toxicity
394 and, ultimately, the production of ROS (*Julkowska & Testerink, 2015*). In our study, PL1 (as the
395 wild-type line) exhibited a dark-purple seed coat and had high levels of anthocyanin, phenolic
396 compounds, and antioxidant activities (*Hong et al., 2019*). Similarly, PL6, which was generated
397 by irradiating PL1 with 200 Gy of gamma rays, also displayed a dark-purple seed coat.

398 As shown in Figure 3D, GSEA revealed several GO terms that were positively correlated with salt
399 stress, including defense response (GO: 0006952), glutathione metabolic process (GO: 0006749),
400 peroxidase activity (GO: 0004601), ROS metabolic process (GO: 0072593), response to biotic
401 stimulus (GO: 0009607), and response to stress (GO:0006950). Among these terms, three were
402 specifically related to antioxidant activity: glutathione metabolic process (GO: 0006749),
403 peroxidase activity (GO: 0004601), and ROS metabolic process (GO: 0072593). These
404 antioxidant-related GO terms are crucial protective mechanisms against salinity stress in plants.
405 Interestingly, we observed that DEGs related to antioxidants were specifically upregulated in PL6
406 48 h after salt stress, despite both PL1 and PL6 having colored seed coats. This suggests that these
407 DEGs may positively contribute to salt stress tolerance, leading to more vigorous shoot and root
408 growth in PL6 than that in PL1. In addition to the gene expression analysis, the measurement of
409 antioxidant enzyme activities further supports the higher antioxidant capacity in PL6 than in PL1
410 under salt stress conditions. CAT and POD activities were significantly increased at 24 and 48 h
411 after salt stress exposure in PL6 (Fig. 7A and B), indicating efficient ROS-scavenging ability and
412 peroxide detoxification, which help protect the cells from oxidative damage during salt stress.
413 Conversely, in PL1, SOD activity slightly decreased at 24 and 48 h post-salt stress (Fig. 7C),
414 suggesting a limited ability to efficiently neutralize superoxide radicals, potentially leading to ROS
415 accumulation and oxidative stress in PL1 under salt stress conditions. Overall, these findings not
416 only provide insights into the DEGs related to antioxidant activity but also highlight the distinctive

417 enzymatic responses to salt stress in PL1 and PL6. The increases in CAT and POD activities and
418 TAC in PL6 might play crucial roles in its superior ability to manage salt-induced oxidative stress
419 compared with the wild-type PL1. The combination of gene expression analysis and antioxidant
420 enzyme activity measurements sheds light on the activation of specific antioxidant pathways in
421 PL6, providing a comprehensive understanding of its enhanced salinity stress response.

422 Phytohormones, such as abscisic acid (ABA) and auxins (indole acetic acid [IAA] and indole-3-
423 butyric acid), play crucial roles in plant responses to environmental stresses, including salinity.
424 ABA is a key signaling molecule involved in the adaptation to salt stress in various crop plants,
425 such as tobacco, alfalfa, common bean, and potato (*Sah et al., 2016*). Meanwhile, IAA contributes
426 to maintaining growth in salt-resistant maize genotypes by regulating shoot turgor and growth
427 through significant increases in shoot sap osmolality (*Zolman & Bartel, 2004; De Costa et al.,*
428 *2007*). In this study, we observed increased transcription levels of TRAESCS1B02G145800 (ABA
429 receptor PYL8) and TRAESCS1B02G138100 (auxin-responsive protein IAA15) in PL6 under salt
430 stress conditions (Table 1). Additionally, salinity-induced osmotic stress leads to the
431 overproduction of ROS and oxidative damage to plant cells. To counteract this, the antioxidant
432 defense system in plants is activated to detoxify ROS and maintain redox homeostasis
433 (*Hasanuzzaman et al., 2021*). Accordingly, we found that plant hormone-related genes, including
434 dehydroascorbate reductase and peroxidase genes, were upregulated in PL6 under salt stress to
435 protect against ROS-induced damage and maintain cellular redox balance (Table 1). The increased
436 expression of ROS-related genes in PL6 suggests that this mutant line may exhibit an altered
437 response to salt stress-induced oxidative stress.

438 In addition to hormone-related responses, transcriptional regulation through histone modification
439 and chromatin remodeling plays a pivotal role in plant responses to salt stress. In this study, we
440 observed an increase in the transcription levels of INO80 complex subunit D
441 (TRAESCS1B02G149000) in PL6 under salt stress conditions. The INO80 chromatin remodeling
442 complex is responsible for evicting the histone variant H2A.Z in eukaryotic cells (*Alatwi & Downs,*
443 *2015*). Studies in *Arabidopsis* have demonstrated that under salt stress, the INO80 complex induces
444 the eviction of H2A.Z-containing nucleosomes from the AtMYB44 promoter region, leading to
445 increased accumulation of AtMYB44 transcripts and thus promoting salt stress tolerance (*Nguyen*
446 *& Cheong, 2018*). However, the specific target gene and position of the histone variant H2A.Z
447 evicted by the INO80 complex in wheat remain unclear. Further investigations are required to
448 identify the precise position of H2A.Z evicted by the INO80 complex and clarify the factors
449 influencing the differential responses of PL1 and PL6 to salinity stress.

450 Moreover, investigation of the MADS-box family members contributes to our understanding of
451 the differential responses of PL1 and PL6 to salinity stress. MADS-box transcription factors are
452 known to regulate flowering development (*Lee & Lee, 2010; Callens et al., 2018*). *Wu et al. (2020)*
453 reported that overexpression of *OsMADS25* in rice and *Arabidopsis* resulted in improved salinity
454 tolerance compared with that in the wild-type. Conversely, the MADS-box transcription factor
455 *AGL16* was identified as a negative regulator of stress responses in *Arabidopsis* (*Zhao et al., 2021*).

456 In this study, we observed increased transcription levels of two MADS-box transcription factors
457 (TRAESCS4A02G002600 and TRAESCS6D02G293200) in PL6 mutant plants under salt stress
458 conditions, suggesting their potential roles in salt tolerance and growth response. These findings
459 provide valuable insights into the molecular mechanisms underlying the differential responses of
460 PL1 and PL6 to salinity.

461 Furthermore, although GO terms related to photosynthesis were detected via GSEA and network
462 analysis (Figs. 3D and 4B), no significant differences were observed in the gene expression
463 patterns between PL1 and PL6. This finding is consistent with the data on chlorophyll
464 concentration (Fig. 2E), which did not show significant variation between PL1 and PL6 during the
465 duration of salt stress exposure. In our previous study, we observed that the total anthocyanin
466 concentrations in wheat mutant lines (used in this study) were significantly higher than those in
467 wild-type lines, resulting in higher antioxidant activity in the mutants compared with the wild-type
468 (*Hong et al., 2019*). In the present study, the enriched factors “Biosynthesis of secondary
469 metabolites” and “Flavonoid biosynthesis” increased following salt stress treatment (Fig. 5). This
470 suggests that the antioxidant activities of PL6 under salt stress conditions might be influenced by
471 these pathways, which include genes associated with GO terms such as glutathione metabolic
472 process (GO: 0006749), peroxidase activity (GO: 0004601), and ROS metabolic process (GO:
473 0072593) (Fig. 3D).

474 As shown in Fig. 4D, several DEGs were mapped to GO terms related to gene expression
475 regulation (GO: 001046), DNA binding transcription factor activity (GO: 0003700), and
476 transcription regulator activity (GO: 0140110). To elucidate the molecular mechanism of salt stress
477 response at the cellular level, we analyzed putative transcription factors and selected those with
478 differential expression patterns in PL6 under salt stress conditions. Among them, the ERF family
479 protein emerged as an important family of transcription factors in plants, regulating various
480 developmental processes (*Ohme-Takagi & Shinshi, 1995*), including their response to salt stress
481 (*Cheng et al., 2013; Li et al., 2020; Trujillo et al., 2008*). Additionally, studies have revealed the
482 significance of the bHLH and MYB gene families in the response to salt stress in plants (*Yang et*
483 *al., 2021; Li et al., 2020; Jiang et al., 2009; Kim et al., 2013; Seo et al., 2012*). The putative
484 transcription factors shown in Fig. 6 can be further analyzed for their functions to better understand
485 the molecular mechanisms of salt response. Flavonoid biosynthesis has been extensively studied
486 and is predominantly regulated at the transcriptional level by the MYB–bHLH–WD40 complex in
487 various plant species, such as rice, *Arabidopsis*, *Mimulus*, apples, and maize (*Tohge et al., 2017;*
488 *An et al., 2020; Yuan et al., 2014; Zheng et al., 2019; Baudry et al., 2006*). In this study, several
489 bHLH and MYB gene families were identified as putative transcription factors, likely influenced
490 by the seed colors of PL1 (wild-type) and PL6 (mutant line) used in the experiment. Consequently,
491 based on the heat map in Fig. 6, the bHLH and MYB gene families exhibiting different expression
492 patterns between PL1 and PL6 were considered differentially expressed transcription factors under
493 salt stress conditions.

494 Moreover, protein kinases play a vital role in regulating plant responses to salt stress. *Singh et al.*
495 (2018) investigated the expression levels of protein kinase genes in response to salt stress in rice
496 plants. They found that two CBL-interacting protein kinases and one MAPK showed more than a
497 two-fold change in PL6 rice lines under salt stress. Similarly, *Xiong et al. (2003)* highlighted the
498 significance of the MAPK gene *OsMPK5* in regulating the salt stress response in rice plants. Apart
499 from MAPKs, other types of protein kinases have also been implicated in salt stress response. For
500 instance, the protein kinase *OsSOS2* is involved in regulating salt tolerance in rice plants by
501 activating the SOS pathway (*Kumar et al., 2022*). Another study reported that the receptor-like
502 kinase *OsWAK35* plays a role in regulating salt stress response in rice plants by activating the
503 MAPK pathway (*Zhang et al., 2005*). These findings underscore the importance of protein kinases
504 in the regulation of plant responses to salt stress and suggest that different types of protein kinases
505 play specific roles in these processes.

506 In the present study, we identified 15 DEGs with more than a two-fold change, among which one,
507 five, and nine genes were involved in the circadian clock system, cytoskeleton organization, and
508 cell wall organization, respectively (Table 3). These processes play crucial roles in plant stress
509 response and are important components of how plants adapt to challenging environments. The
510 circadian clock system has been found to be essential in regulating the plant's response to salt
511 stress. *Xu et al. (2022)* conducted a study on *Arabidopsis* plants and demonstrated that the circadian
512 clock system is involved in the modulation of salt stress responses. They observed altered
513 expression levels of circadian clock genes under salt stress conditions and further noted that the
514 disruption of the circadian clock system resulted in reduced salt tolerance in the plants. Likewise,
515 the cytoskeleton organization is also critical for regulating plant responses to salt stress. For
516 instance, in rice plants, the actin cytoskeleton has been shown to play a role in regulating the
517 response to salt stress, ion homeostasis, and ROS scavenging (*Chun et al., 2021*). Disruption of
518 the actin filaments in rice plants led to reduced salt tolerance, indicating the importance of the
519 cytoskeleton in coping with salt-induced stress. Moreover, the cell wall organization is a vital
520 aspect of the response of maize to salt stress. A study on maize revealed that the expression of
521 genes related to the cell wall was altered under salt stress conditions, and modification of the cell
522 wall composition contributed to increased salt tolerance in the plants (*Oliveira et al., 2020*). These
523 findings highlight the significance of the cell wall in mediating the plant's ability to withstand salt
524 stress.

525 The primary focus of this study was to investigate the molecular mechanisms underlying salinity
526 stress responses in the colored wheat mutant PL6 through transcriptomic profiling of leaf tissues.
527 However, considering the crucial role of roots in nutrient and mineral absorption, examining the
528 variations in Na^+ and K^+ levels in root tissues could provide valuable insights into tissue-specific
529 ion absorption and accumulation mechanisms in PL6. Furthermore, conducting a comprehensive
530 analysis of DEGs in root tissues could reveal novel genes and pathways associated with salt stress
531 responses that significantly contribute to the enhanced tolerance observed in PL6. Further research
532 incorporating histological analyses of root tissues and transcriptomic profiling of roots would be

533 instrumental in unraveling the genetic basis and tissue-level adaptations responsible for the
534 superior salt stress response and tolerance of PL6.

535 In summary, this investigation of the effects of salinity stress on two wheat lines, namely PL1
536 (wild-type) and PL6 (mutant line generated through gamma irradiation of PL1), revealed that salt
537 stress negatively affected germination and plant growth in both lines. However, PL6 demonstrated
538 greater tolerance to salinity stress than PL1, indicating that the mutant line has acquired
539 mechanisms to more effectively mitigate salt stress-induced damage. The differences in ion
540 concentrations observed in PL6, including lower Na⁺ levels and higher K⁺ levels, suggest better
541 ion homeostasis in this line, contributing to its enhanced salt stress tolerance. Our genome-wide
542 transcriptomic analysis provided insights into the differential expression patterns of genes between
543 PL1 and PL6 under salt stress conditions, leading to the observed phenotypic differences. Several
544 GO terms related to defense responses, glutathione metabolism, peroxidase activity, and ROS
545 metabolic processes were positively correlated with salt stress, highlighting the importance of
546 antioxidant activities in salt tolerance. The specific upregulation of DEGs related to antioxidants
547 in PL6, despite both lines having colored seed coats, suggests that these DEGs play critical roles
548 in enhancing salt stress tolerance and promoting vigorous shoot and root growth. Additionally,
549 hormone-related genes, transcription factors, and protein kinases displayed differential expression,
550 indicating their involvement in the differential salt stress responses between PL1 and PL6. The
551 enrichment of pathways related to flavonoid biosynthesis and secondary metabolite biosynthesis
552 in PL6 further suggests their contribution to the enhanced antioxidant activities observed in this
553 line. It is important to acknowledge that the mechanisms underlying salt stress resistance in plants
554 are highly complex and not easily discernible. The interplay of various genetic, physiological, and
555 biochemical factors contributes to the overall response to salinity stress, making it challenging to
556 draw straightforward conclusions. Nevertheless, understanding these intricate mechanisms is
557 crucial for developing stress-tolerant crop varieties and improving agricultural practices. By
558 gaining insights into the genes and pathways responsible for salt stress tolerance, researchers can
559 design targeted breeding programs to develop salt-resistant crop varieties, thereby enhancing
560 global food production and addressing food security challenges.

561

562 **Conclusions**

563 In conclusion, this study provides valuable information on the differential responses of the wheat
564 lines PL1 and PL6 to salinity stress. The identification of various genes and pathways associated
565 with salt stress tolerance in PL6 offers promising avenues for further research and potential
566 applications in crop improvement. As we continue to unravel the intricate network of stress-
567 tolerant mechanisms in plants, we move closer to the goal of developing resilient and productive
568 agricultural systems to ensure food security in the face of environmental challenges. Because PL6
569 was developed through mutation breeding, it can be used as a breeding parent or genetic material.
570 Mutation breeding is a technique used to increase genetic diversity by inducing mutations through
571 exposure to radiation, chemical agents, or other mutagenic factors, and it is widely used for rapid

572 and effective plant improvement. Because of mutagenesis in PL6, it possesses distinct
573 characteristics from its original parent PL1 and exhibits higher tolerance to environmental stresses,
574 displaying different responses from PL1. The traits resulting from this mutation are stably inherited
575 genetically, making PL6 a valuable genetic resource that can be used as a breeding parent or
576 crossed with other genetic materials to develop new genotypes. Consequently, PL6 represents an
577 important genetic resource for enhancing agricultural productivity and food security, and through
578 further research and development, it can be effectively used to explore more efficient uses of plant
579 genetic resources and contribute to the development of new plant varieties.

580

581 **Data Availability Statement**

582 The FASTQ files of raw data has been submitted to NCBI Sequence Read Archive (SRA), and the
583 SRA accession is PRJNA937396

584

585 **References**

586 **Al-Ashkar I, Alderfasi A, El-Hendawy S, Al-Suhaibani N, El-Kafafi S, Seleiman M. 2019.**
587 Detecting salt tolerance in doubled haploid wheat lines. *Agronomy* **9(4)**:211 DOI
588 10.3390/agronomy9040211.

589 **Alatwi HE, Downs JA. 2015.** Removal of H2A.Z by INO80 promotes homologous
590 recombination. *EMBO Reports* **16(8)**:986–994 DOI 10.15252/embr.201540330.

591 **Amirbakhtiar N, Ismaili A, Ghaffari MR, Nazarian Firouzabadi F, Shobbar ZS. 2019.** Transcriptome
592 response of roots to salt stress in a salinity-tolerant bread wheat cultivar. *PLOS ONE* **14(3)**:e0213305 DOI
593 10.1371/journal.pone.0213305.

594 **An JP, Wang XF, Zhang XW, Xu HF, Bi SQ, You CX, Hao YJ. 2020.** An apple Myb
595 transcription factor regulates cold tolerance and anthocyanin accumulation and undergoes
596 Miell-mediated degradation. *Plant Biotechnology Journal* **18(2)**:337–353 DOI
597 10.1111/pbi.13201.

598 **Anders S, Pyl PT, Huber W. 2015.** Htseq—A python framework to work with high-throughput
599 sequencing data. *Bioinformatics* **31(2)**: 166–169 DOI 10.1093/bioinformatics/btu638.

600 **Asif MA, Schilling RK, Tilbrook J, Brien C, Dowling K, Rabie H, Short L, et al. 2018.**
601 Mapping of novel salt tolerance QTL in an Excalibur × Kukri doubled haploid wheat population.
602 TAG. *Theoretical and Applied Genetics* **131**:2179–2196 DOI 10.1007/s00122-018-3146-y.

603 **Baudry A, Caboche M, Lepiniec L. 2006.** Tt8 controls its own expression in a feedback
604 regulation involving Ttg1 and homologous Myb and bHLH factors, allowing a strong and
605 cell-specific accumulation of flavonoids in *Arabidopsis thaliana*. *The Plant Journal* **46(5)**:768–
606 779 DOI 10.1111/j.1365-313X.2006.02733.x.

607 **Callens C, Tucker MR, Zhang D, Wilson ZA. 2018.** Dissecting the role of MADS-box genes in
608 monocot floral development and diversity. *Journal of Experimental Botany* **69(10)**: 2435–2459
609 DOI 10.1093/jxb/ery086.

- 610 **Chele KH, Tinte MM, Piater LA, Dubery IA, Tugizimana F. 2021.** Soil salinity, a serious
611 environmental issue and plant responses: A metabolomics perspective. *Metabolites* **11(11):724**
612 DOI 10.3390/metabo11110724.
- 613 **Chen Z, Pottosin II, Cuin TA, Fuglsang AT, Tester M, Jha D, Zepeda-Jazo I, Zhou M,**
614 **Palmgren MG, Newman IA, Shabala S. 2007.** Root plasma membrane transporters controlling
615 K⁺/Na⁺ homeostasis in salt-stressed barley. *Plant Physiology* **145(4):1714–1725** DOI
616 10.1104/pp.107.110262.
- 617 **Cheng MC, Liao PM, Kuo WW, Lin TP. 2013.** The Arabidopsis ethylene response Factor1
618 regulates abiotic stress-responsive gene expression by binding to different cis-acting elements in
619 response to different stress signals. *Plant Physiology* **162(3):1566–1582** DOI
620 10.1104/pp.113.221911.
- 621 **Choudhary A, Kaur N, Sharma A, Kumar A. 2021.** Evaluation and screening of elite wheat
622 germplasm for salinity stress at the seedling phase. *Physiologia Plantarum* **173(4):2207–2215** DOI
623 10.1111/ppl.13571.
- 624 **Chun HJ, Baek D, Jin BJ, Cho HM, Park MS, Lee SH, Lim LH, Cha YJ, Bae DW, Kim ST,**
625 **Yun DJ, Kim MC. 2021.** Microtubule dynamics plays a vital role in plant adaptation and tolerance
626 to salt stress. *International Journal of Molecular Sciences* **22(11):5957** DOI
627 10.3390/ijms22115957.
- 628 **Colmer T D, Flowers, T J, Munns R. 2006.** Use of wild relatives to improve salt tolerance in
629 wheat. *Journal of Experimental Botany* **57(5):1059–1078** DOI 10.1093/jxb/erj124.
- 630 **Craig Plett D, Møller IS. 2010.** Na⁽⁺⁾ transport in glycophytic plants: What we know and would
631 like to know. *Plant, Cell & Environment* **33(4):612–626** DOI 10.1111/j.1365-3040.2009.02086.x.
- 632 **Assaha DVM, Ueda A, Saneoka H, Al-Yahyai R, Yaish MW. 2017.** The role of Na⁺ and K⁺
633 transporters in salt stress adaptation in glycophytes. *Frontiers in Physiology* **8:509** DOI
634 10.3389/fphys.2017.00509.
- 635 **De Costa W, Zörb C, Hartung W, Schubert S. 2007.** Salt resistance is determined by osmotic
636 adjustment and abscisic acid in newly developed maize hybrids in the first phase of salt stress.
637 *Physiologia Plantarum* **131(2):311–321** DOI 10.1111/j.1399-3054.2007.00962.x.
- 638 **Deinlein U, Stephan AB, Horie T, Luo W, Xu G, Schroeder J I. 2014.** Plant salt-tolerance
639 mechanisms. *Trends in Plant Science* **19(6):371–379** DOI 10.1016/j.tplants.2014.02.001.
- 640 **El-Hendawy S. E, Hassan WM, Al-Suhaibani NA, Refay Y, Abdella KA. 2017.** Comparative
641 performance of multivariable agro-physiological parameters for detecting salt tolerance of wheat
642 cultivars under simulated saline field growing conditions. *Frontiers in Plant Science* **8:435** DOI
643 10.3389/fpls.2017.00435.
- 644 **El-Hendawy S, Elshafei A, Al-Suhaibani N, Alotabi M, Hassan W, Dewir YH, Abdella K.**
645 **2019.** Assessment of the salt tolerance of wheat genotypes during the germination stage based on
646 germination ability parameters and associated SSR markers. *Journal of Plant Interactions*
647 **14(1):151–163** DOI 10.1080/17429145.2019.1603406.

- 648 **EL Sabagh A, Islam MS, Skalicky M, Ali Raza M, Singh K, Anwar Hossain M, et al. 2021.**
649 Salinity stress in wheat (*Triticum aestivum* L.) in the changing climate: Adaptation and
650 management strategies. *Frontiers in Agronomy* **3**:661932 DOI 10.3389/fagro.2021.661932.
- 651 **Genç Y, Taylor J, Lyons G, Li Y, Cheong J, Appelbee M, Oldach K, Sutton T. 2019.** Bread wheat
652 with high salinity and sodicity tolerance. *Frontiers in Plant Science* **10**:1280 DOI:
653 10.3389/fpls.2019.01280.
- 654 **Hanin M, Ebel C, Ngom M, Laplaze L, Masmoudi K. 2016.** New insights on plant salt tolerance
655 mechanisms and their potential use for breeding. *Frontiers in Plant Science* **7**:1787 DOI
656 10.3389/fpls.2016.01787.
- 657 **Hasanuzzaman M, Alam MM., Rahman A, Hasanuzzaman M, Nahar K, Fujita M. 2014.**
658 Exogenous proline and glycine betaine mediated upregulation of antioxidant defense and
659 glyoxalase systems provides better protection against salt-induced oxidative stress in two rice
660 (*Oryza sativa* L.) varieties. *BioMed Research International* **2014**:757219 DOI
661 10.1155/2014/757219.
- 662 **Hasanuzzaman M, Raihan MRH, Masud AAC, Rahman K, Nowroz F, Rahman M, Nahar
663 K, Fujita M. 2021.** Regulation of reactive oxygen species and antioxidant defense in plants under
664 salinity. *International Journal of Molecular Sciences* **22(17)**:9326 DOI 10.3390/ijms22179326.
- 665 **Hong MJ, Kim DY, Nam BM, Ahn JW, Kwon SJ, Seo YW, Kim JB. 2019.** Characterization
666 of novel mutants of hexaploid wheat (*Triticum aestivum* L.) with various depths of purple grain
667 color and antioxidant capacity. *Journal of the Science of Food and Agriculture* **99(1)**:55–63 DOI
668 10.1002/jsfa.9141.
- 669 **Horie T, Hause, F, Schroeder JI. 2009.** HKT transporter-mediated salinity resistance
670 mechanisms in *Arabidopsis* and monocot crop plants. *Trends in Plant Science* **14(12)**:660–668
671 DOI 10.1016/j.tplants.2009.08.009.
- 672 **Huang S, Spielmeyer W, Lagudah ES, Munns, R. 2008.** Comparative mapping of HKT genes
673 in wheat, barley, and rice, key determinants of Na⁺ transport, and salt tolerance. *Journal of*
674 *Experimental Botany* **59(4)**:927–937. DOI: 10.1093/jxb/ern033.
- 675 **Hussain N, Ghaffar A, Zafar ZU, Javed M, Shah KH, Noreen S, Manzoor H, Iqbal M,
676 Hassan IFZ, Bano H, Gul HS, Aamir M, Khalid A, Sohail Y, Ashraf M, Athar H. U. R. 2021.**
677 Identification of novel source of salt tolerance in local bread wheat germplasm using morpho-
678 physiological and biochemical attributes. *Scientific Reports* **11**:10854. DOI 10.1038/s41598-021-
679 90280-w.
- 680 **Ismail AM, Horie T. 2017.** Genomics, physiology, and molecular breeding approaches for
681 improving salt tolerance. *Annual Review of Plant Biology* **68**:405–434. DOI 10.1146/annurev-
682 arplant-042916-040936.
- 683 **Jiang Y, Yang B, Deyholos MK. 2009.** Functional characterization of the *Arabidopsis* bHLH92
684 transcription factor in abiotic stress. *Molecular Genetics and Genomics* **282**:503–516. DOI
685 10.1007/s00438-009-0481-3.
- 686 **Julkowska MM, Testerink C. 2015.** Tuning plant signaling and growth to survive salt. *Trends in*
687 *Plant Science* **20(9)**:586–594. DOI 10.1016/j.tplants.2015.06.008.

- 688 **Kim D, Langmead B, Salzberg SL. 2015.** HISAT: A fast spliced aligner with low memory
689 requirements. *Nature Methods* **12**:357–360. DOI 10.1038/nmeth.3317.
- 690 **Kim JH, Nguyen NH, Jeong CY, Nguyen NT, Hong SW, Lee H. 2013.** Loss of the R2r3 Myb,
691 Atmyb73, causes hyper-induction of the Sos1 and Sos3 genes in response to high salinity in
692 *Arabidopsis*. *Journal of Plant Physiology* **170(16)**:1461–1465 DOI 10.1016/j.jplph.2013.05.011.
- 693 **Kissoudis C, van de Wiel C, Visser RGF, van der Linden G. 2014.** Enhancing crop resilience
694 to combined abiotic and biotic stress through the dissection of physiological and molecular
695 crosstalk. *Frontiers in Plant Science* **5**:207 DOI 10.3389/fpls.2014.00207.
- 696 **Kumar P, Sharma PK. 2020.** Soil salinity and food security in India. *Frontiers in Sustainable*
697 *Food Systems* **4**:533781 DOI 10.3389/fsufs.2020.533781.
- 698 **Lee J, Lee I. 2010.** Regulation and function of SOC1, a flowering pathway integrator. *Journal of*
699 *Experimental Botany* **61(9)**:2247–2254. DOI 10.1093/jxb/erq098.
- 700 **Lichtenthaler HK. 1987.** Chlorophyll and carotenoids: Pigments of photosynthetic
701 biomembranes. *Methods in Enzymology* **148**:350–382 DOI 10.1016/0076-6879(87)48036-1.
- 702 **Li H., Xu G, Yang C, Yang L, Liang Z. 2019.** Genome-wide identification and expression
703 analysis of HKT transcription factor under salt stress in nine plant species. *Ecotoxicology and*
704 *Environmental Safety* **171**:435–442 DOI 10.1016/j.ecoenv.2019.01.008..
- 705 **Li J, Zhu L, Hull J J, Liang S, Daniell, H Jin S, Zhang X. 2016.** Transcriptome analysis reveals
706 a comprehensive insect resistance response mechanism in cotton to infestation by the phloem
707 feeding insect Bemisia tabaci (whitefly). *Plant Biotechnology Journal* **14(10)**:1956–1975 DOI
708 10.1111/pbi.12554.
- 709 **Li J, Wang T, Han J, Ren Z. 2020.** Genome-wide identification and characterization of cucumber
710 bHLH family genes and the functional characterization of CsbHLH041 in NaCl and Aba tolerance
711 in *Arabidopsis* and cucumber. *BMC Plant Biology* **20**:272 DOI 10.1186/s12870-020-02440-1.
- 712 **Li WY, Wang C, Shi HH, Wang B, Wang J. X, Liu YS, Ma JY, Tian SY, Zhang YW. 2020.**
713 Genome-wide analysis of ethylene-response factor family in adzuki Bean and functional
714 determination of Vaerf3 under saline-alkaline stress. *Plant Physiology and Biochemistry* **147**:215–
715 222 DOI 10.1016/j.plaphy.2019.12.019.
- 716 **Lloyd A, Brockman A, Aguirre L, Campbell A, Bean A, Cantero A, Gonzalez A. 2017.**
717 Advances in the Myb–bHLH–Wd repeat (MBW) pigment regulatory model: Addition of a Wrky
718 factor and Co-option of an anthocyanin Myb for betalain regulation. *Plant & Cell Physiology*
719 **58(9)**:1431–1441. DOI: 10.1093/pcp/pcx075
- 720 **Long W, Zou X, Zhang X. 2015.** Transcriptome analysis of canola (*Brassica napus*) under salt
721 stress at the germination stage. *PLOS ONE* **10(2)**:e0116217. DOI: 10.1371/journal.pone.0116217
- 722 **Luo H, Huo P, Wang Z, Zhang S, He Z, Wu Y, Zhao L, Liu J, Guo J, Fang S, Cao W, Yi L,**
723 **Zhao Y, Kong L. 2021.** KOBAS-i: Intelligent prioritization and exploratory visualization of
724 biological functions for gene enrichment analysis. *Nucleic Acids Research* **49(W1)**:W317–W325.
725 DOI: 10.1093/nar/gkab447

- 726 **Merico D, Isserlin R, Stueker O, Emili A, Bader GD. 2010.** Enrichment map: A network-based method
727 for gene-set enrichment visualization and interpretation. *PLOS ONE*, **5(11)**:e13984 DOI:
728 10.1371/journal.pone.0013984
- 729 **Møller IS, Tester M. 2007.** Salinity tolerance of *Arabidopsis*: A good model for cereals? *Trends*
730 *in Plant Science* 12(12):534–540 DOI 10.1016/j.tplants.2007.09.009.
- 731 **Møller IS, Gilliham M, Jha D, Mayo GM, Roy SJ, Coates JC, Haseloff J, Tester M. 2009.**
732 Shoot Na⁺ exclusion and increased salinity tolerance engineered by cell type-specific alteration of
733 Na⁺ transport in *Arabidopsis*. *Plant Cell* **21(7)**:2163–2178 DOI 10.1105/tpc.108.064568.
- 734 **Munns R, James RA, Xu B, Athman A, Conn SJ., Jordans C, Byrt CS, Hare RA, Tyerman**
735 **SD, Tester M, Plett D, Gilliham M. 2012.** Wheat grain yield on saline soils is improved by an
736 ancestral Na⁺ transporter gene. *Nature Biotechnology* **30**:360–364 DOI 10.1038/nbt.2120.
- 737 **Munns R, Tester M. 2008.** Mechanisms of salinity tolerance. *Annual Review of Plant Biology*
738 **59**:651–681 DOI 10.1146/annurev.arplant.59.032607.092911. **Nguyen NH, Cheong JJ. 2018.**
739 H2A.Z-containing nucleosomes are evicted to activate AtMYB44 transcription in response to salt
740 stress. *Biochemical Biophysical Research Communications* **499(4)**:1039–1043 DOI
741 10.1016/j.bbrc.2018.04.048.
- 742 **Nieves-Cordones, M., Al Shiblawi, F. R., & Sentenac, H. 2016.** Roles and transport of sodium
743 and potassium in plants. In *The alkali metal ions: Their role for life* (pp. 291–324). Springer. doi:
744 10.1007/978-3-319-21756-7_9.
- 745 **Ohme-Takagi M, Shinshi H. 1995.** Ethylene-inducible DNA binding proteins that interact with
746 an ethylene-responsive element. *Plant Cell* **7(2)**:173–182 DOI 10.1105/tpc.7.2.173.
- 747 **Omrani S, Arzani A, Esmailzadeh Moghaddam ME, Mahlooji M. 2022.** Genetic analysis of
748 salinity tolerance in wheat (*Triticum aestivum* L.). *PLOS ONE* **17(3)**:e0265520 DOI
749 10.1371/journal.pone.0265520.
- 750 **Oliveira DM, Mota TR, Salatta FV, Sinzker RC, Končítiková R, Kopečný D, Dos Santos WD.**
751 **2020.** Cell wall remodeling under salt stress: Insights into changes in polysaccharides,
752 feruloylation, lignification, and phenolic metabolism in maize. *Plant Cell & Environment* **43(9)**:
753 2172-2191 DOI: [10.1111/pce.13805](https://doi.org/10.1111/pce.13805)
- 754 **Peng Z, He S, Gong W, Sun J, Pan Z, Xu F, Lu Y, Du X. 2014.** Comprehensive analysis of
755 differentially expressed genes and transcriptional regulation induced by salt stress in two
756 contrasting cotton genotypes. *BMC Genomics* **15**:760 DOI 10.1186/1471-2164-15-760.
- 757 **Raudvere U, Kolberg L, Kuzmin I, Arak T, Adler P, Peterson H, Vilo JG. 2019.** g:Profiler: A web
758 server for functional enrichment analysis and conversions of gene lists (2019 update). *Nucleic Acids*
759 *Research* **47(W1)**:W191–W198 DO: 10.1093/nar/gkz369.
- 760 **Riedelsberger J, Miller JK, Valdebenito-Maturana B, Piñeros MA, González W, Dreyer I.**
761 **2021.** Plant HKT channels: An updated view on structure, function and gene regulation.
762 *International Journal of Molecular Sciences* **22(4)**:1892 DOI 10.3390/ijms22041892.

- 763 **Robinson MD, McCarthy DJ, Smyth GK. 2010.** Edger: A bioconductor package for differential
764 expression analysis of digital gene expression data. *Bioinformatics* **26(1)**:139–140 DOI
765 10.1093/bioinformatics/btp616.
- 766 **Saade S, Brien C, Pailles Y, Berger B, Shahid M, Russell J, Waugh R, Negrão S, Tester M.**
767 **2020.** Dissecting new genetic components of salinity tolerance in two-row spring barley at the
768 vegetative and reproductive stages. *PLOS ONE* **15(7)**:e0236037 DOI
769 10.1371/journal.pone.0236037.
- 770 **Sadak M S. 2019.** Physiological role of trehalose on enhancing salinity tolerance of wheat plant.
771 *Bulletin of National Research Centre* **43**:53 DO: 10.1186/s42269-019-0098-6.
- 772 **Sah SK, Reddy KR, Li J. 2016.** Abscisic acid and abiotic stress tolerance in crop plants. *Frontiers*
773 *in Plant Science* **7**:571 DOI 10.3389/fpls.2016.00571.
- 774 **Sayed HI. 1985.** Diversity of salt tolerance in a germplasm collection of wheat (*Triticum* spp.).
775 *Theoretical and Applied Genetics* **69**:651–657 DOI 10.1007/BF00251118.
- 776 **Schachtman DP, Schroeder JI. 1994.** Structure and transport mechanism of a high-affinity
777 potassium uptake transporter from higher plants. *Nature* **370(6491)**:655–658 DOI
778 10.1038/370655a0.
- 779 **Seleiman M, Talha Aslam M, Ahmed Alhammad B, Umair Hassan M, Maqbool R, Umer**
780 **Chattha M, Khan I, Ileri Gitari H, S Uslu O, Roy R, Leonardo Battaglia M. 2022.** Salinity
781 Stress in Wheat: Effects, Mechanisms and Management Strategies. *Phyton-International Journal*
782 *of Experimental Botany* **91(4)**:667–694 DOI: 10.32604/phyton.2022.017365.
- 783 **Seo JS, Sohn HB, Noh K, Jung C, An JH, Donovan CM, Somers DA, Kim DI, Jeong SC, Kim**
784 **CG, Kim HM, Lee S, Choi YD, Moon TW, Kim CH, Cheong J. 2012.** Expression of the
785 Arabidopsis Atmyb44 gene confers drought/salt-stress tolerance in transgenic soybean. *Molecular*
786 *Breeding* **29**:601–608 DOI 10.1007/s11032-011-9576-8.
- 787 **Shavrukov Y, Langridge P, Tester M. 2009.** Salinity tolerance and sodium exclusion in genus
788 *Triticum*. *Breeding Science* **59(5)**:671–678. DOI 10.1270/jsbbs.59.671.
- 789 **Shiferaw B, Smale M, Braun HJ, Duveiller E, Reynolds M, Muricho G. 2013.** Crops that feed
790 the world 10. Past successes and future challenges to the role played by wheat in global food
791 security. *Food Security* **5**:291–317 DOI 10.1007/s12571-013-0263-y.
- 792 **Singh V, Singh A., Bhadoria J, Giri J, Singh J, TV V, Sharma, PC. 2018.** Differential
793 expression of salt-responsive genes to salinity stress in salt-tolerant and salt-sensitive rice (*Oryza*
794 *sativa* L.) at seedling stage. *Protoplasma* **255**:1667-1681 DOI 10.1007/s00709-018-1257-6
- 795 **Singh DP, Sarkar RK. 2014.** Distinction and characterisation of salinity tolerant and sensitive
796 rice cultivars as probed by the chlorophyll fluorescence characteristics and growth parameters.
797 *Functional Plant Biology* **41(7)**:727–736 DOI 10.1071/FP13229.
- 798 **Sreenivasulu N, Usadel B, Winter A, Radchuk V, Scholz U, Stein N, Weschke W, Strickert M, Close**
799 **TJ, Stitt M, Graner A, Wobus U. 2008.** Barley grain maturation and germination: Metabolic pathway

- 800 and regulatory network commonalities and differences highlighted by new MapMan/PageMan profiling
801 tools. *Plant Physiology* **146(4)**:1738–1758 DOI 10.1104/pp.107.111781.
- 802 **Subramanian A, Tamayo P, Mootha VK, Mukherjee S, Ebert BL, Gillette MA, Paulovich A, Pomeroy**
803 **SL, Golub TR, Lander ES, Mesirov JP. 2005.** Gene set enrichment analysis: A knowledge-based
804 approach for interpreting genome-wide expression profiles. *Proceedings of the National Academy*
805 *of Sciences* **102(43)**:15545–15550 DOI 10.1073/pnas.0506580102.
- 806 Tester M, Davenport R. 2003. Na⁺ tolerance and Na⁺ transport in higher plants. *Annals of Botany*
807 **91(5)**:503–527 DOI 10.1093/aob/mcg058.
- 808 **Tian F, Yang DC, Meng YQ, Jin J, Gao G. 2020.** Plantregmap: Charting functional regulatory
809 maps in plants. *Nucleic Acids Research* **48(D1)**:D1104–D1113 DOI 10.1093/nar/gkz1020.
- 810 **Tohge T, de Souza LP, Fernie AR. 2017.** Current understanding of the pathways of flavonoid
811 biosynthesis in model and crop plants. *Journal of Experimental Botany* **68(15)**:4013–4028 DOI
812 10.1093/jxb/erx177.
- 813 **Trujillo LE, Sotolongo M, Menéndez C, Ochogavía ME, Coll Y, Hernández I, Borrás-**
814 **Hidalgo O, Thomma BP, Vera P, Hernández L. 2008.** Soderf3, a novel sugarcane ethylene
815 responsive factor (erf), enhances salt and drought tolerance when overexpressed in tobacco plants.
816 *Plant & Cell Physiology* **49(4)**:512–525 DOI 10.1093/pcp/pcn025.
- 817 **Tsai YC, Chen KC, Cheng TS, Lee C, Lin SH, Tung CW. 2019.** Chlorophyll fluorescence
818 analysis in diverse rice varieties reveals the positive correlation between the seedlings salt
819 tolerance and photosynthetic efficiency. *BMC Plant Biology* **19**:403 DOI 10.1186/s12870-019-
820 1983-8.
- 821 **Vera Alvarez R, Pongor LS, Mariño-Ramírez L, Landsman D. 2019.** Tpmcalculator: One-step
822 software to quantify mRNA abundance of genomic features. *Bioinformatics* **35(11)**:1960–1962
823 DOI 10.1093/bioinformatics/bty896.
- 824 **Wu J, Yu C, Hunag L, Wu M, Liu B, Liu Y, Song G, Liu D, Gan Y. 2020.** Overexpression of
825 MADS-box transcription factor OsMADS25 enhances salt stress tolerance in Rice and
826 Arabidopsis. *Plant Growth Regulation* **90**:163–171 DOI 10.1007/s10725-019-00539-6.
- 827 .
- 828 **Yang Q, Chen ZZ, Zhou X F, Yin HB, Li X, Xin XF, Hong XH, Zhu JK, Gong Z. 2009.**
829 Overexpression of SOS (salt overly sensitive) genes increases salt tolerance in transgenic
830 Arabidopsis. *Molecular Plant* **2(1)**:22–31 DOI 10.1093/mp/ssn058.
- 831 **Yang YY, Zheng PF, Ren YR, Yao YX, You CX, Wang XF, Hao YJ. 2021.** Apple Mdsat1
832 encodes a bHLHm1 transcription factor involved in salinity and drought responses. *Planta* **253**:46
833 DOI 10.1007/s00425-020-03528-6.
- 834 **Yuan YW, Sagawa JM, Frost L, Vela JP, Bradshaw HD Jr. 2014.** Transcriptional control of
835 floral anthocyanin pigmentation in monkeyflowers (*Mimulus*). *New Phytologist* **204(4)**:1013–
836 1027 DOI 10.1111/nph.12968.

- 837 **Zhang, S., Chen, C., Li, L., Meng, L., Singh, J., Jiang, N., & Lemaux, P. G.** 2005. Evolutionary
838 expansion, gene structure, and expression of the rice wall-associated kinase gene family. *Plant*
839 *Physiology* **139(3)**:1107-1124 DOI [1107-1124](https://doi.org/10.1104/pp.105.069005). [10.1104/pp.105.069005](https://doi.org/10.1104/pp.105.069005).
- 840 **Zhang Y, Fang J, Wu X. Na Dong L** 2018. Na⁺/K⁺ balance and transport Regulatory mechanisms
841 in weedy and cultivated rice (*Oryza sativa* L.) under salt stress. *BMC Plant Biology* **18**:375 DOI
842 [10.1186/s12870-018-1586-9](https://doi.org/10.1186/s12870-018-1586-9).
- 843 **Zhao PX, Zhang J, Chen SY, Wu J, Xia JQ, Sun LQ, Ma SS, Xiang CB.** 2021. Arabidopsis
844 MADS-box factor AGL16 is a negative regulator of plant response to salt stress by downregulating
845 salt-responsive genes. *New Phytologist* **232(6)**:2418–2439 DOI [10.1111/nph.17760](https://doi.org/10.1111/nph.17760).
- 846 **Zheng J, Wu H, Zhu H, Huang C, Liu C, Chang Y, Kong Z, Zhou Z, Wang G, Lin Y, Chen**
847 **H.** 2019. Determining factors, regulation system, and domestication of anthocyanin biosynthesis
848 in rice leaves. *New Phytologist* **223(2)**:705–721 DOI [10.1111/nph.15807](https://doi.org/10.1111/nph.15807).
- 849 **Zolman BK, Bartel B.** 2004. An Arabidopsis indole-3-butyric acid-response mutant defective in
850 PEROXIN6, an apparent ATPase implicated in peroxisomal function. *Proceedings of the National*
851 *Academy of Sciences* **101(6)**:1786–1791 DOI [10.1073/pnas.0304368101](https://doi.org/10.1073/pnas.0304368101).

852 **Figure titles and legends**

853 **Figure 1. Effect of salt stress on seed germination and seedling growth.**

854 (A) Germination rate of wheat seeds under different salt concentrations. 500 seeds from each line
855 were placed on two layers of germination paper and exposed to a solution containing 150mM NaCl
856 in a phytohealth chamber (SPL Life Sciences) at a temperature of 22°C. Germination was assessed
857 after 4 days. (B) Wheat seedling growth under different salinity levels. Seven-day-old seedlings
858 were subjected to a salt stress treatment with a total volume of 200ml of the solution containing
859 150mM NaCl after 4 days. (C) Phenotypes of wheat seedlings under different salinity levels after
860 4 days of salt stress with a total volume of 200ml of the solution containing 150mM NaCl. (D)
861 Shoot and root lengths of wheat seedlings under different salinity conditions after 4 days of salt
862 stress with a total volume of 200ml of the solution containing 150mM NaCl. Independent t-tests
863 demonstrated significant differences (* $p < 0.05$ and ** $p < 0.01$).

864

865 **Figure 2. Na⁺ and K⁺ ion contents, differential ratios of K⁺ and Na⁺ and chlorophyll** 866 **concentrations for PL1 and PL6 under salt stress treatment.**

867 Seven-day-old seedlings were subjected to a salt stress treatment with a total volume of 200ml of
868 the solution containing 150mM NaCl. After treatment with 150 mM NaCl, wheat leaves were
869 collected at 3, 24, and 48 hours. (A) Na⁺ ion content in the shoots under different salt stress
870 exposure times. (B) K⁺ ion content in the shoots under different salt stress exposure times. (C)
871 Changes in the relative "Na⁺ ratio" in shoots at different time points after salt stress treatment. The
872 "Na⁺ ratio" represents the relative proportion of Na⁺ content in shoots compared to the Na⁺
873 content at 0 hours (baseline). Data points at 3 hours, 24 hours, and 48 hours indicate the fold
874 change of Na⁺ content in shoots compared to the baseline (0 hours). (D) Changes in the relative
875 "K⁺ ratio" in shoots at different time points after salt stress treatment. The "K⁺ ratio" represents
876 the relative proportion of K⁺ content in shoots compared to the K⁺ content at 0 hours (baseline).
877 Data points at 3 hours, 24 hours, and 48 hours indicate the fold change of K⁺ content in shoots
878 compared to the baseline (0 hours). (E) Chlorophyll concentrations in the shoots under different
879 salt stress exposure times. Each bar represents the mean \pm standard error (n = 3). Independent t-
880 tests showed significant differences (* $p < 0.05$ and ** $p < 0.01$).

881

882 **Figure 3. Differentially expressed genes (DEGs) and Gene Set Enrichment Analysis (GSEA)** 883 **for PL1 and PL6.**

884 (A) Venn diagrams showing the number of DEGs between PL1 and PL6 and the overlap of all
885 DEGs at different time points after exposure to salt stress. (B) Number of DEGs only expressed in
886 PL1 at different time points after exposure to salt stress. (C) Number of DEGs only expressed in
887 PL6 at different time points after exposure to salt stress. (D) GSEA enrichment analysis with gene
888 ontology of the DEGs. Dots indicate significant GO terms from the pairwise gene set enrichment
889 analysis comparisons at each time point after exposure to salt stress. The size of the dots indicates
890 the number of genes, and the color of the dots indicates the $-\log_{10}$ FDR value within the pathway.

891

892 **Figure 4. Gene ontology (GO) Enrichment Map and differential gene expression profiling** 893 **for PL1 and PL6.**

894 (A–E) Five networks of significantly enriched gene sets between PL1 and PL6 obtained on the
895 Enrichment Map. Nodes representing enriched gene sets were classified based on their similarity
896 to related gene sets. The size of the node is proportional to the total number of genes. The thickness
897 of the green line between nodes represents the proportion of shared genes between gene sets. (F–

898 J) The expression patterns of each network at each time point after exposure to salt stress. Each
899 cluster represents a group of functionally related gene sets that showed similar expression patterns.
900 Figure 4F, 4G, 4H, 4I, and 4J show multiple clusters derived from the networks of Figures 4A,
901 4B, 4C, 4D, and 4E, respectively. Clusters showing different expression patterns between PL1 and
902 PL6 were indicated in red boxes. (K) Heatmaps representing the expressions of differentially
903 expressed genes (DEGs) marked in red boxes (F, G, and I) for PL1 and PL6.

904

905 **Figure 5. Gene Set Enrichment Analysis with Kyoto Encyclopedia of Genes and Genomes**
906 **(KEGG) pathways of the differentially expressed genes (DEGs).**

907 Dots represent significant KEGG pathways from the pairwise gene set enrichment analysis
908 comparisons at each time point after exposure to salt stress. The size of the dots indicates the
909 number of differential genes, while the color of the dots represents the p-values of enrichment
910 analysis. The rich factor refers to the ratio of the number of DEGs in the pathway to the total
911 number of genes. The size of the dots indicates the number of genes, and the color of the dots
912 indicates the $-\log_{10}$ FDR value within the pathway.

913

914 **Figure 6. Differentially expressed transcription factors (TFs) under salt stress treatment in**
915 **PL1 and PL6.**

916 (A) Distribution of TF family members among the differentially expressed genes (DEGs). The bar
917 graph illustrates the number of TFs belonging to each TF family among the DEGs. (B) Expression
918 patterns of TFs at each time point after exposure to salt stress. Each cluster with similar expression
919 patterns is indicated by red boxes. (C) Heatmap analysis of TF family genes in PL1 and PL6 under
920 salt stress treatment, with the genes marked by red boxes in (B) specifically highlighted.

921

922 **Figure 7. Biochemical assays of antioxidant enzyme activity.**

923 (A) Catalase (CAT) activity, (B) Peroxidase (POD) activity, (C) Total Superoxide Dismutase
924 (SOD) activity, and (D) Total Antioxidant Capacity (TAC). Each bar represents the average \pm
925 standard error ($n = 3$). Independent t-tests demonstrated significant differences ($* p < 0.05$ and $**$
926 $p < 0.01$) compared to the control condition (0h).

927

928 **Figure 8. Validation of the RNA sequencing results via reverse transcription-quantitative**
929 **polymerase chain reaction (RT-qPCR) at different timepoints under salt stress conditions.**

930 Three clusters representing different expression patterns for PL1 and PL6 were selected and the
931 relative expressions shown. RT-qPCR was performed with three biological replicates. Each bar
932 represents the average \pm standard error ($n = 3$). Independent t-tests showed significant differences
933 ($* p < 0.05$ and $** p < 0.01$)

934

935 **Supplemental information Titles and Legends**

936 **Supplementary Figure 1 (Fig. S1). Field images of M6 generations of PL1 and PL6 at**
937 **different time points.**

938 (A) Plot images of M6 generations of PL1 and PL6 at different time points. (B) and (C) Different
939 views of the field at various time points. The dates when the photos were taken are indicated below
940 each image.

941

942 **Supplementary Figure 2 (Fig. S2). Comparison of seed coat color of different wheat lines.**

943 PL1 (control) and PL6 (mutant lines) were used in this study. Additionally, Chengwoo and
944 Keumkang are two of the cultivars commonly grown in South Korea.

945

946 **Supplementary Figure 3 (Fig. S3). Comparison of salt stress response in mutant lines (PL2-
947 PL49) and wild type control (PL1).**

948 (A) Germination rate of mutant lines (PL2-PL49) and PL1 as the wild type control. (B) Shoot
949 length of mutant lines (PL2-PL49) and PL1 as the wild type control. (C) Root length of mutant
950 lines (PL2-PL49) and PL1 as the wild type control. For the preliminary screening of the selected
951 mutant lines, 100 seeds from each line were placed in a phytohealth chamber (SPL Life Sciences)
952 with two layers of germination paper, and a total volume of 200ml of the solution containing
953 150mM NaCl was applied to them at a temperature of 22°C. After 4 days, the germination rate,
954 shoot length, and root length were recorded. PL1 served as the wild type control in these
955 experiments.

956

957 **Supplementary Table 1 (Table S1). The details of the primers used in this study.**

958

959 **Supplementary Table 2 (Table S2). Germination ratio the different salt concentrations on
960 seed germination.**

961

962 **Supplementary Table 3 (Table S3). Summary of RNA-seq quality, read counts, and mapping
963 rates.**

964

965 **Supplementary Table 4 (Table S4). Differentially expressed genes (DEGs) from BlastX
966 results against NCBI Poaceae family.**

967 This table contains the blastx results against the NCBI *Poaceae* family, which led to the
968 identification of a total of 4,017 differentially expressed genes (DEGs) with a p-value < 0.05 and
969 FDR < 0.05.

970

971 **Supplementary Table 5 (Table S5). Gene Set Enrichment Analysis (GSEA) for PL1 and PL6
972 using gene ontology (GO) mapping of differentially expressed genes.**

973

974 **Supplementary Table 6 (Table S6). Gene Set Enrichment Analysis (GSEA) for PL1 and PL6
975 using Kyoto Encyclopedia of Genes and Genomes (KEGG) pathways mapping of
976 differentially expressed genes.**

977

978 **Supplementary Table 7 (Table S7). Differentially express genes in red boxes of Fig. 6B used
979 in Fig. 6C.**

980

Figure 1

Figure 1. Effect of salt stress on seed germination and seedling growth.

(A) Germination rate of wheat seeds under different salt concentrations. 500 seeds from each line were placed on two layers of germination paper and exposed to a solution containing 150mM NaCl in a phytohealth chamber (SPL Life Sciences) at a temperature of 22°C. Germination was assessed after 4 days. (B) Wheat seedling growth under different salinity levels. Seven-day-old seedlings were subjected to a salt stress treatment with a total volume of 200ml of the solution containing 150mM NaCl after 4 days. (C) Phenotypes of wheat seedlings under different salinity levels after 4 days of salt stress with a total volume of 200ml of the solution containing 150mM NaCl. (D) Shoot and root lengths of wheat seedlings under different salinity conditions after 4 days of salt stress with a total volume of 200ml of the solution containing 150mM NaCl. Independent t-tests demonstrated significant differences (* $p < 0.05$ and ** $p < 0.01$).

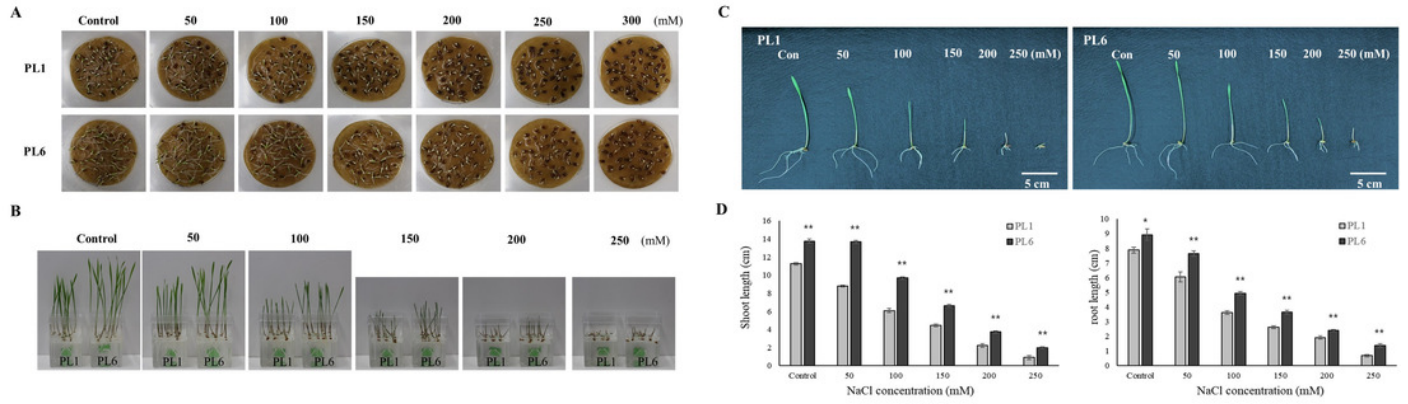


Figure 2

Figure 2. Na⁺ and K⁺ ion contents, differential ratios of K⁺ and Na⁺ and chlorophyll concentrations for PL1 and PL6 under salt stress treatment.

Seven-day-old seedlings were subjected to a salt stress treatment with a total volume of 200ml of the solution containing 150mM NaCl. After treatment with 150 mM NaCl, wheat leaves were collected at 3, 24, and 48 hours. (A) Na⁺ ion content in the shoots under different salt stress exposure times. (B) K⁺ ion content in the shoots under different salt stress exposure times. (C) Changes in the relative "Na⁺ ratio" in shoots at different time points after salt stress treatment. The "Na⁺ ratio" represents the relative proportion of Na⁺ content in shoots compared to the Na⁺ content at 0 hours (baseline). Data points at 3 hours, 24 hours, and 48 hours indicate the fold change of Na⁺ content in shoots compared to the baseline (0 hours). (D) Changes in the relative "K⁺ ratio" in shoots at different time points after salt stress treatment. The "K⁺ ratio" represents the relative proportion of K⁺ content in shoots compared to the K⁺ content at 0 hours (baseline). Data points at 3 hours, 24 hours, and 48 hours indicate the fold change of K⁺ content in shoots compared to the baseline (0 hours). (E) Chlorophyll concentrations in the shoots under different salt stress exposure times. Each bar represents the mean \pm standard error (n = 3). Independent t-tests showed significant differences (* $p < 0.05$ and ** $p < 0.01$).

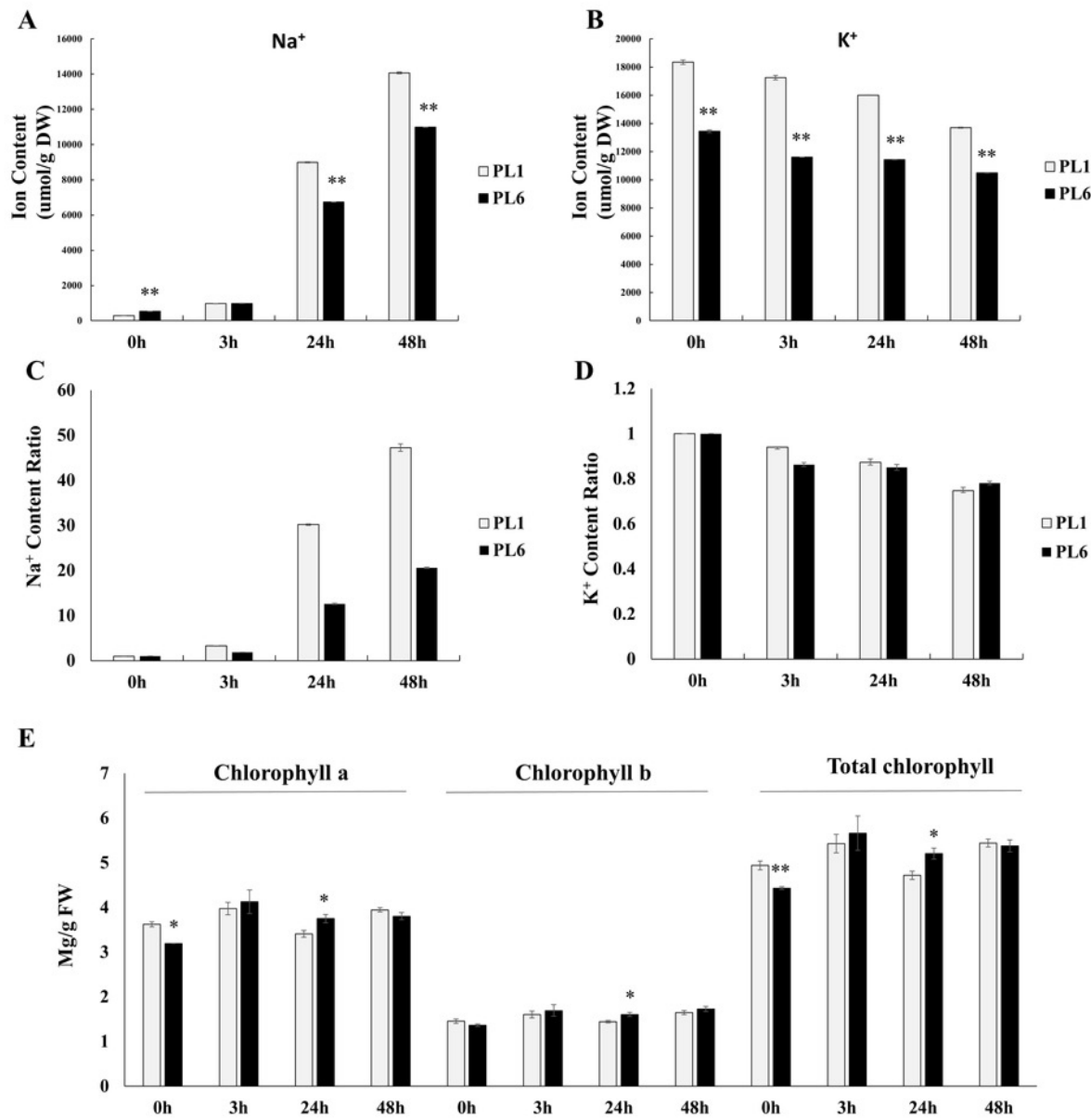


Figure 3

Figure 3. Differentially expressed genes (DEGs) and Gene Set Enrichment Analysis (GSEA) for PL1 and PL6.

(A) Venn diagrams showing the number of DEGs between PL1 and PL6 and the overlap of all DEGs at different time points after exposure to salt stress. (B) Number of DEGs only expressed in PL1 at different time points after exposure to salt stress. (C) Number of DEGs only expressed in PL6 at different time points after exposure to salt stress. (D) GSEA enrichment analysis with gene ontology of the DEGs. Dots indicate significant GO terms from the pairwise gene set enrichment analysis comparisons at each time point after exposure to salt stress. The size of the dots indicates the number of genes, and the color of the dots indicates the $-\log_{10}$ FDR value within the pathway.

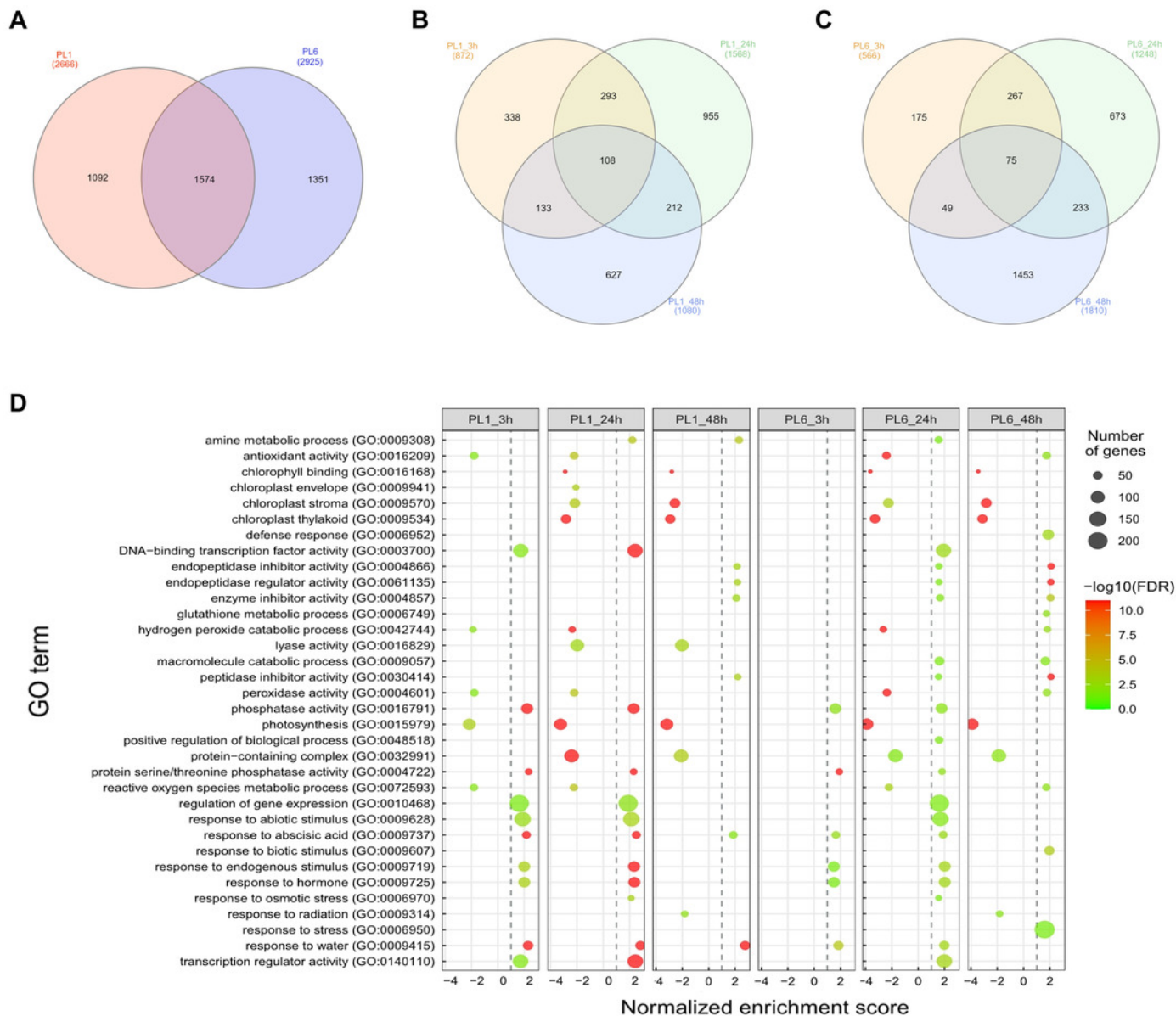


Figure 4

Figure 4. Gene ontology (GO) Enrichment Map and differential gene expression profiling for PL1 and PL6.

(A-E) Five networks of significantly enriched gene sets between PL1 and PL6 obtained on the Enrichment Map. Nodes representing enriched gene sets were classified based on their similarity to related gene sets. The size of the node is proportional to the total number of genes. The thickness of the green line between nodes represents the proportion of shared genes between gene sets. (F-J) The expression patterns of each network at each time point after exposure to salt stress. Each cluster represents a group of functionally related gene sets that showed similar expression patterns. Figure 4F, 4G, 4H, 4I, and 4J show multiple clusters derived from the networks of Figures 4A, 4B, 4C, 4D, and 4E, respectively. Clusters showing different expression patterns between PL1 and PL6 were indicated in red boxes. (K) Heatmaps representing the expressions of differentially expressed genes (DEGs) marked in red boxes (F, G, and I) for PL1 and PL6.

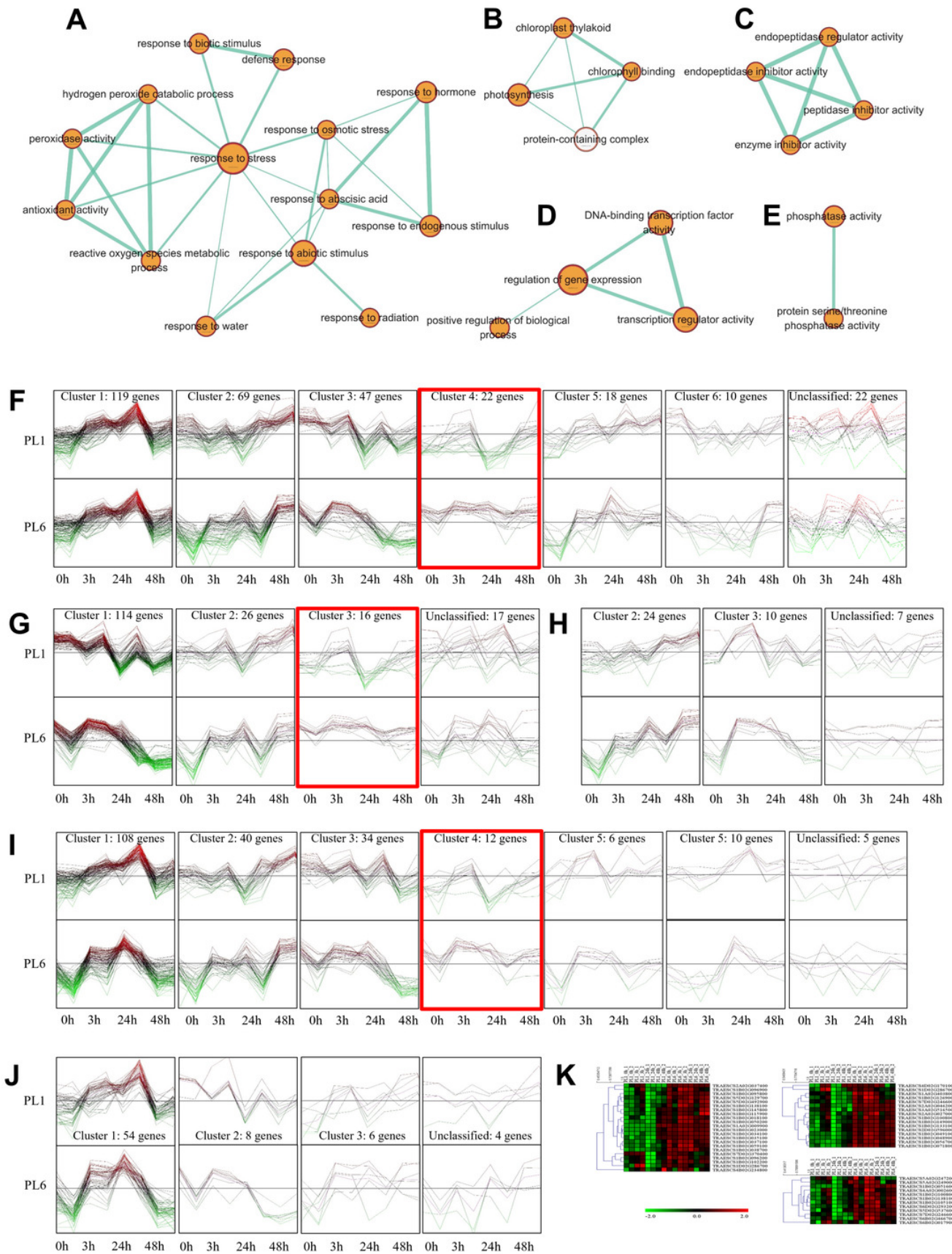


Figure 5

Figure 5. Gene Set Enrichment Analysis with Kyoto Encyclopedia of Genes and Genomes (KEGG) pathways of the differentially expressed genes (DEGs).

Dots represent significant KEGG pathways from the pairwise gene set enrichment analysis comparisons at each time point after exposure to salt stress. The size of the dots indicates the number of differential genes, while the color of the dots represents the p-values of enrichment analysis. The rich factor refers to the ratio of the number of DEGs in the pathway to the total number of genes. The size of the dots indicates the number of genes, and the color of the dots indicates the $-\log_{10}$ FDR value within the pathway.

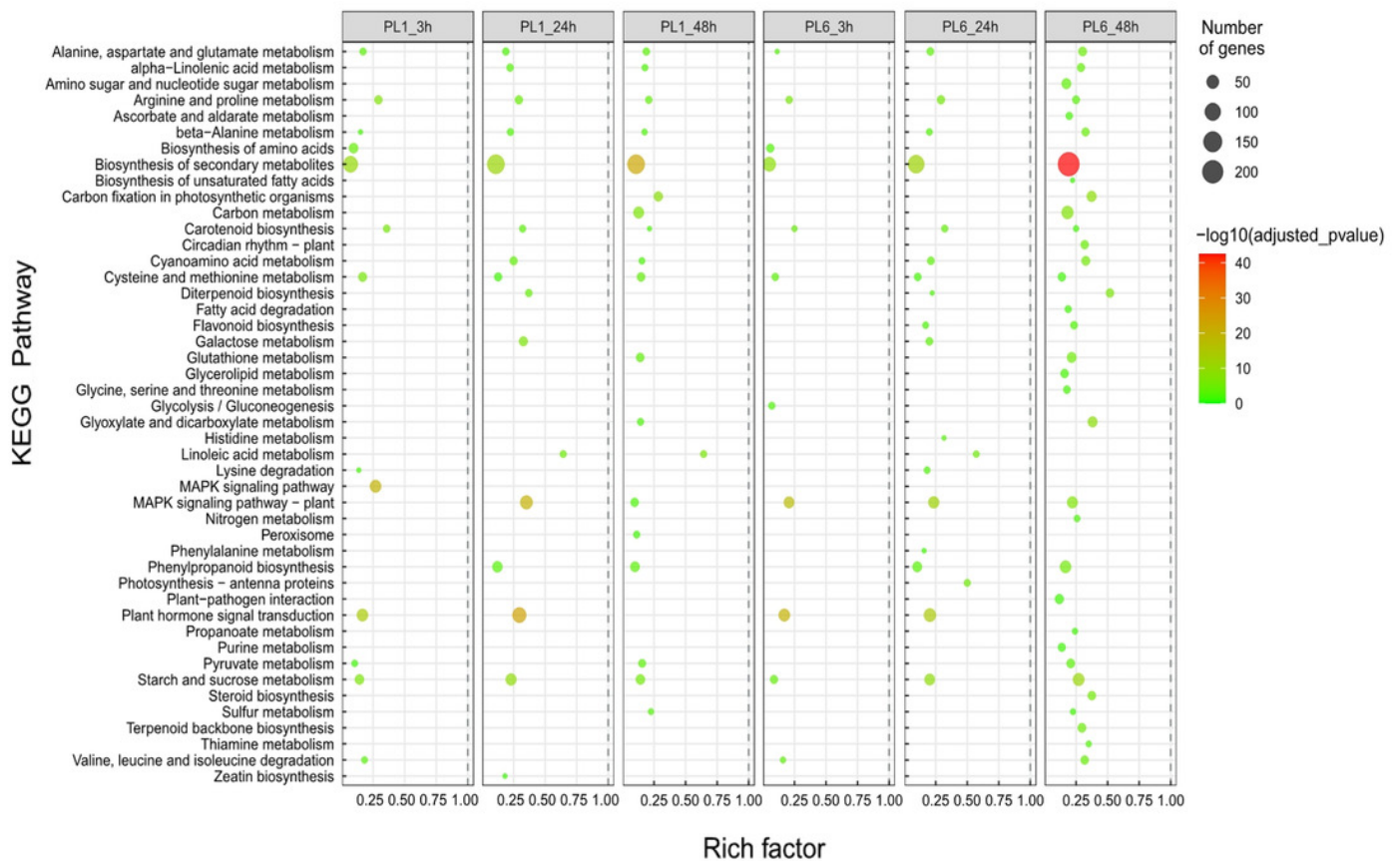


Figure 6

Figure 6. Differentially expressed transcription factors (TFs) under salt stress treatment in PL1 and PL6.

(A) Distribution of TF family members among the differentially expressed genes (DEGs). The bar graph illustrates the number of TFs belonging to each TF family among the DEGs. (B) Expression patterns of TFs at each time point after exposure to salt stress. Each cluster with similar expression patterns is indicated by red boxes. (C) Heatmap analysis of TF family genes in PL1 and PL6 under salt stress treatment, with the genes marked by red boxes in (B) specifically highlighted.

Figure 7

Figure 7. Biochemical assays of antioxidant enzyme activity.

(A) Catalase (CAT) activity, (B) Peroxidase (POD) activity, (C) Total Superoxide Dismutase (SOD) activity, and (D) Total Antioxidant Capacity (TAC). Each bar represents the average \pm standard error ($n = 3$). Independent t-tests demonstrated significant differences (* $p < 0.05$ and ** $p < 0.01$) compared to the control condition (0h).

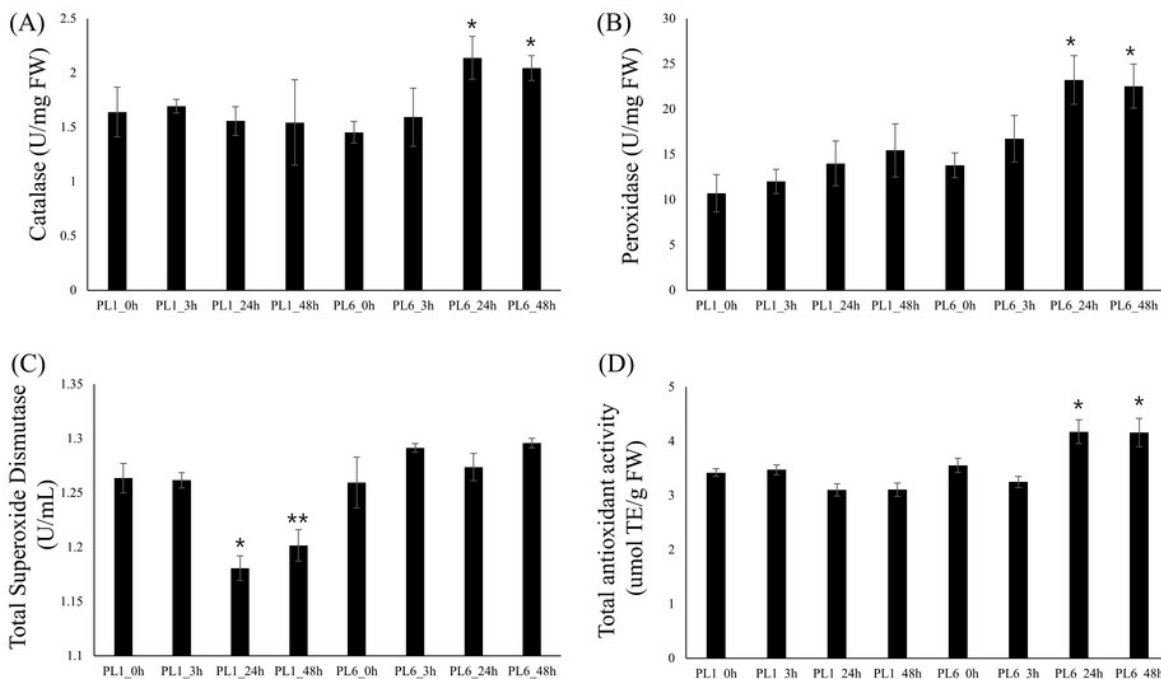


Figure 8

Figure 8. Validation of the RNA sequencing results via reverse transcription-quantitative polymerase chain reaction (RT-qPCR) at different timepoints under salt stress conditions.

Three clusters representing different expression patterns for PL1 and PL6 were selected and the relative expressions shown. RT-qPCR was performed with three biological replicates. Each bar represents the average \pm standard error ($n = 3$). Independent t-tests showed significant differences (* $p < 0.05$ and ** $p < 0.01$)

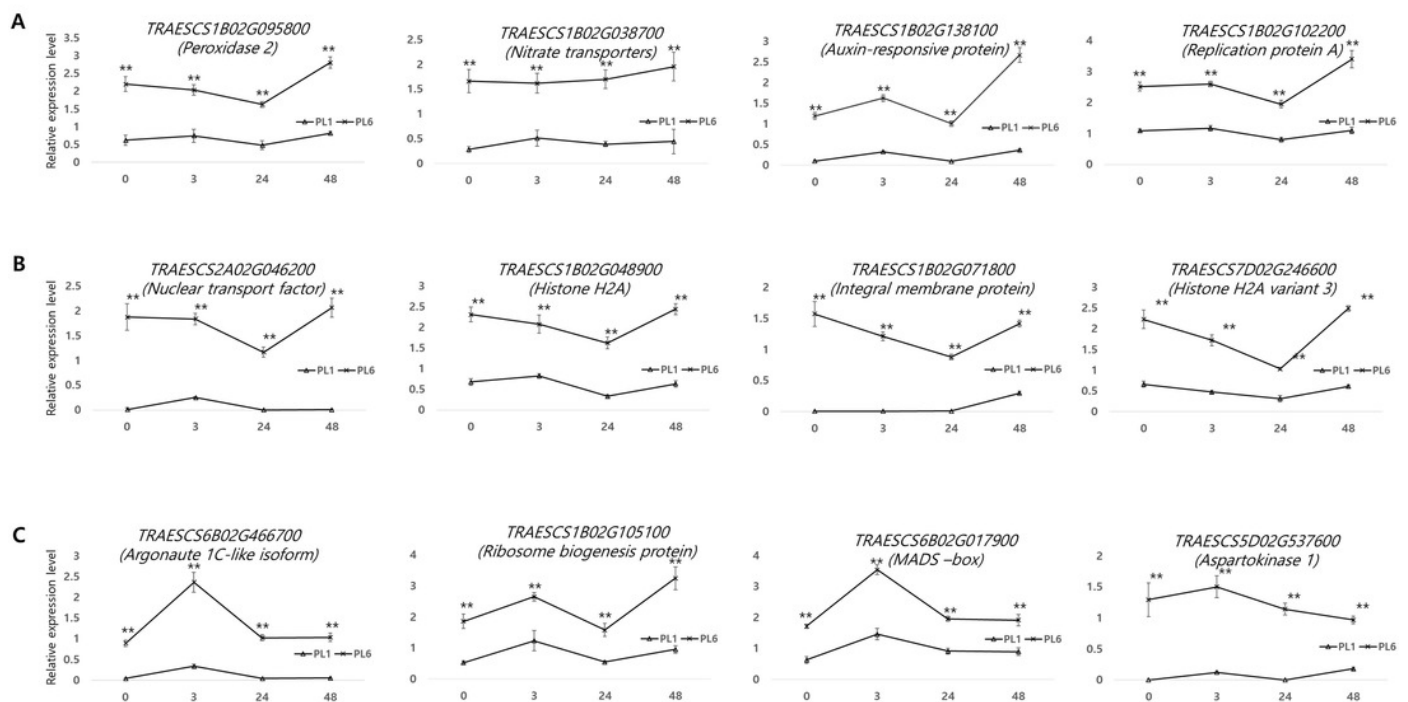


Table 1 (on next page)

Table 1. List of differentially expressed genes selected by K-means clustering from GSEA analysis

1 **Table 1:**2 **List of differentially expressed genes selected by K-means clustering from GSEA analysis.**

Gene ID	Description	Length	E-value	Similarity (%)	Log2 fold change (PL6/PL1)				p-value	FDR	Group
					0 h	3 h	12 h	24 h			
TRAESCS1B02G145800	abscisic acid receptor PYL8	205	1E-149	92.57	4.37	1.96	7.28	1.87	2.09E-19	2.53E-29	
TRAESCS1B02G138100	auxin-responsive protein IAA15	198	2E-143	81.71	3.64	1.88	3.57	2.42	1.56E-28	6.22E-36	
TRAESCS5D02G129700	chaperone protein dnaJ GFA2, mitochondrial	421	0	84.11	8.75	1.57	6.56	5.69	4.77E-38	7.45E-69	
TRAESCS1B02G018100	defensin	81	1.1E-38	84.72	4.86	7.74	5.55	-0.43	1.82E-09	4.81E-93	
TRAESCS1B02G059100	dehydroascorbate reductase	212	9E-156	95.77	3.75	3.64	3.78	1.76	4.05E-69	4.52E-24	DEGs in red boxes
TRAESCS1B02G050200	E3 ubiquitin-protein ligase XB3	486	0	82.96	3.96	3.92	4.48	1.15	1.98E-36	9.28E-17	of cluster 4
TRAESCS5D02G492900	heat shock cognate 70 kDa protein 2	614	0	92.5	3.67	1.74	3.52	3.68	6.04E-97	2.97E-66	in Fig. 4F
TRAESCS1B02G037100	NAD(P)-binding Rossmann-fold superfamily protein	300	0	91.03	5.36	4.72	5.49	2.27	5.67E-67	1.12E-26	
TRAESCS1B02G095800	Peroxidase 2	340	0	89.71	7.85	1.71	7.13	2.85	8.69E-72	9.78E-22	
TRAESCS1B02G096200	peroxidase 5	338	0	85.36	4.99	1.58	4.80	1.88	1.81E-23	3.68E-64	
TRAESCS1B02G096900	Peroxidase 5	343	0	75.36	4.34	1.12	3.82	3.15	7.29E-26	8.91E-18	
TRAESCS1B02G115900	peroxidase A2-like	342	0	82.95	3.84	2.45	4.16	3.27	5.42E-59	3.96E-69	
TRAESCS1B02G038700	protein NRT1/ PTR FAMILY 6.2	582	0	90.52	7.36	8.20	8.09	1.46	1.78E-64	2.32E-34	
TRAESCS1A02G009900	putative disease resistance RPP13-like protein 3	844	0	82.63	6.88	6.49	6.40	-1.81	1.3E-14	2.22E-56	

TRAESCS1B02G023000	putative disease resistance RPP13-like protein 3	920	0	72.15	7.98	8.61	7.67	2.83	2.09E-29	9.97E-62	
TRAESCS1B02G102200	replication protein A 70 kDa DNA-binding subunit C-like	881	0	73.55	4.59	0.95	7.35	2.00	2.3E-18	1.6E-27	
TRAESCS2A02G037400	stress-response A/B barrel domain-containing protein HS1	115	9E-76	85.48	8.11	1.65	8.58	8.10	2.94E-31	2.53E-29	
TRAESCS1B02G034100	subtilisin-chymotrypsin inhibitor CI-1B	74	1.8E-44	84.47	9.97	11.00	11.50	3.89	4.45E-72	3.44E-77	
TRAESCS1B02G035100	subtilisin-chymotrypsin inhibitor CI-1B	74	2.3E-45	84.72	10.70	11.55	12.07	2.56	2.35E-80	4.03E-13	
TRAESCS4D02G170100	60S ribosomal protein L19-1	228	2E-144	88.22	7.03	-0.34	7.73	-7.05	5.65E-47	1.2E-44	
TRAESCS2A02G027000	actin-related protein 9 isoform X1	526	0	84.59	5.48	1.33	3.59	2.19	6.68E-81	1.05E-77	
TRAESCS1B02G133100	DNA-directed RNA polymerases II, IV and V subunit 11	119	2E-86	96.77	8.01	2.08	8.31	2.82	7.37E-23	3.82E-21	
TRAESCS2D02G596000	exocyst complex component EXO70A1	637	0	93.63	6.65	2.49	5.61	2.78	7.27E-83	1.44E-79	DEGs
TRAESCS1B02G048900	histone H2A	154	1E-99	92.72	5.66	5.03	6.05	3.09	2.91E-11	6.97E-10	in red boxes
TRAESCS1B02G049100	histone H2A	155	1E-98	91.26	7.65	8.17	8.49	3.42	4.73E-34	4.76E-32	of cluster 3
TRAESCS1D02G286700	histone H4	103	6.6E-70	99.76	3.41	-1.75	2.65	0.70	6.57E-35	6.97E-33	in Fig. 4G
TRAESCS1B02G149000	INO80 complex subunit D	288	0	82.89	7.67	1.69	7.82	2.84	6.2E-18	3.82E-21	
TRAESCS1B02G126900	NAD(P)H-quinone oxidoreductase subunit S, chloroplastic	239	6E-167	82.95	3.54	1.97	3.25	1.86	3.85E-37	2.43E-16	
TRAESCS2A02G046200	nuclear transport factor 2 (NTF2)-	199	4E-	82.59	8.80	2.01	8.64	8.71	6.74E-30	6.97E-33	

	like protein		115								
TRAESCS1A02G403800	predicted protein	266	0	96.99	2.85	2.44	2.78	1.30	0.006931	1.05E-77	
TRAESCS7D02G370400	predicted protein	312	0	83.35	2.11	-0.21	3.22	2.03	8.65E-36	5.3E-28	
TRAESCS7D02G246600	probable histone H2A variant 3	139	3E-95	95.7	2.08	1.78	3.65	2.75	1.62E-42	1.44E-79	
TRAESCS3A02G516500	Protein COFACTOR ASSEMBLY OF COMPLEX C SUBUNIT B CCB3, chloroplastic	192	4E-117	76.6	7.91	2.26	8.02	8.40	4.51E-69	3.25E-66	
TRAESCS1B02G100800	RNA-binding protein 8A	209	9E-152	85.74	4.77	1.01	4.64	2.08	7.57E-28	1.2E-44	
TRAESCS1B02G071800	thylakoid membrane protein TERC, chloroplastic	377	0	84.39	9.49	8.95	9.08	1.70	3.6E-18	2.67E-40	
TRAESCS1B02G056700	translation initiation factor IF-2 isoform X1	239	7E-174	78.99	6.41	8.58	5.77	2.58	5.67E-56	9.72E-34	
TRAESCS5D02G537600	aspartokinase 1, chloroplastic-like	596	0	68.69	8.62	4.45	9.11	1.84	1.63E-37	2.03E-35	
TRAESCS1B02G138100	auxin-responsive protein IAA15	198	2E-143	81.71	3.64	1.88	3.57	2.42	1.56E-28	1.12E-26	
TRAESCS5A02G247200	glucose-6-phosphate isomerase 1, chloroplastic	614	0	93.86	3.08	1.57	2.09	-0.27	2.07E-28	2.68E-36	DEGs in red boxes
TRAESCS4A02G002600	MADS-box transcription factor 47-like isoform X2	163	7E-116	92.93	3.95	0.66	2.60	3.05	0.000023	0.000247	of cluster 4
TRAESCS7D02G246600	probable histone H2A variant 3	139	3E-95	95.7	2.08	1.78	3.65	2.75	5.65E-47	1.47E-26	in Fig. 4I
TRAESCS6B02G466700	protein argonaute 1C-like isoform X2	1013	0	89.28	5.24	2.58	4.52	5.89	1.53E-64	8.82E-62	
TRAESCS6D02G293200	putative MADS-domain transcription factor	228	1E-167	96.69	5.72	2.42	6.37	2.55	1.46E-42	1.31E-43	
TRAESCS1B02G100800	RNA-binding protein 8A	209	9E-152	85.74	4.77	1.01	4.64	2.08	4.73E-34	2.42E-40	

TRAESCS1B02G105100	ribosome biogenesis protein NOP53	407	0	83.3	4.30	1.07	6.42	2.08	2.01E-38	4.76E-32	<hr/>
TRAESCS1B02G051600	uncharacterized protein LOC109787361	466	0	62.52	6.65	9.45	5.94	3.47	6.62E-46	1.2E-44	

3 **Bold numbers indicate more than two-fold changes in expression.**

Table 2 (on next page)

Table 2. List of diiferentially expressed protein kinase genes under salt stress condition

1 **Table 2:**2 **List of differentially expressed protein kinase genes under salt stress condition.**

Gene ID	Description	Length	E-value	Similarity (%)	Log ₂ fold change (PL6/PL1)				p-value	FDR
					0 h	3 h	12 h	24 h		
TraesCS1B02G098700	CBL-interacting protein kinase 17	466	0	89.58	5.64	1.70	4.46	1.42	3.76E-43	6.32E-41
TraesCS5B02G223900	CBL-interacting protein kinase 16	447	0	88.69	0.66	0.32	-0.20	-0.80	0.00187	0.011796
TraesCS4B02G319900	CBL-interacting protein kinase 9	443	0	94.32	1.37	0.71	0.36	0.35	4.87E-26	3.05E-24
TraesCS1B02G098600	CBL-interacting protein kinase 17	466	0	89.63	5.45	1.75	6.91	0.84	2.73E-25	1.65E-23
TraesCS5A02G492000	CBL-interacting protein kinase 9	446	0	94.25	0.72	0.47	0.04	0.28	8.66E-13	2.34E-11
TraesCS1D02G082500	CBL-interacting protein kinase 17	480	0	87.23	-0.21	0.29	-0.62	-0.89	3.29E-05	0.000341
TraesCS4D02G118500	CBL-interacting protein kinase 14	362	0	82.78	0.67	1.11	0.31	0.33	0.00488	0.026029
TraesCS1D02G082600	CBL-interacting protein kinase 17	448	0	86.72	0.36	0.01	-0.50	-0.37	6.13E-05	0.000598
TraesCS1A02G080600	CBL-interacting protein kinase 17	466	0	90.22	-0.39	-0.16	-0.76	-1.21	1.96E-07	0.000003
TraesCS1A02G080700	CBL-interacting protein kinase 17	471	0	89.6	-0.26	0.23	-0.86	-0.50	1.12E-10	2.52E-09
TraesCS4B02G120400	CBL-interacting protein kinase 14	444	0	92.95	-0.12	-0.80	0.86	0.38	0.000271	0.002245
TraesCS2D02G107100	CBL-interacting protein kinase 29	436	0	87.67	-0.24	-0.31	-0.51	0.08	0.005552	0.02886
TraesCS3B02G169300	CBL-interacting protein kinase 5	464	0	93.17	0.61	0.96	0.16	-0.54	4.65E-08	7.74E-07
TraesCS4D02G316500	CBL-interacting protein kinase 9	445	0	94.22	1.03	0.96	-0.10	0.27	3.23E-12	8.38E-11
TraesCS3D02G151500	CBL-interacting protein kinase 5	464	0	93.02	0.59	0.71	0.13	-0.26	2.39E-05	0.000254
TraesCS3A02G135500	CBL-interacting protein kinase 5	466	0	92.32	1.13	0.05	0.14	0.00	4.62E-06	5.69E-05
TraesCS1B02G104900	mitogen-activated protein kinase 14	549	0	92.96	3.98	1.64	3.09	1.98	6.05E-42	9.68E-40
TraesCS7A02G410700	mitogen-activated protein kinase 12	578	0	92.91	0.41	0.32	0.07	0.55	7.32E-06	8.69E-05

TraesCS5B02G075800	SNF1-type serine-threonine protein kinase	363	0	93.99	0.85	0.85	0.20	0.92	5.49E-05	0.000542
TraesCS5D02G081700	SNF1-type serine-threonine protein kinase	364	0	94.37	0.54	0.77	0.22	0.52	0.000294	0.002407
TraesCS1D02G308200	SNF1-related protein kinase regulatory subunit beta-1	280	0	82.88	-1.25	-0.65	0.17	0.67	7.37E-05	0.000706
TraesCS5A02G069500	SNF1-type serine-threonine protein kinase	360	0	95.18	-0.78	-0.29	-0.35	0.67	0.002772	0.01638

3 Bold numbers indicate more than two-fold changes in expression.

Table 3 (on next page)

Table 3. List of differentially expressed salt stress responsive genes selected by MapMan program

1 **Table 3:**2 **List of differentially expressed salts stress responsive genes selected by MapMan program.**

Gene ID	Description	Length	E-value	Similarity (%)	Log ₂ fold change (PL6/PL1)				p-value	FDR	BinName from MapMan
					0 h	3 h	12 h	24 h			
TraesCSU02G196100	Pseudo-response regulator (PRR)	660	0	97.11	-0.67	-0.01	-0.99	-4.44	4.11E-07	5.98E-06	Circadian clock system
TraesCS5D02G078500	Kinesin-like protein KIN-12F isoform X2	3015	0	84.6	-0.73	-0.21	-0.05	-2.42	7.62E-15	2.4E-13	Cytoskeleton organization
TraesCS1B02G123200	Kinesin-like protein KIN-13A	519	0	92.31	5.27	2.00	5.67	2.61	1.73E-62	8.72E-60	Cytoskeleton organization
TraesCS1B02G024500	Actin-7	377	0	99.58	4.70	4.81	5.63	2.86	4.55E-63	2.37E-60	Cytoskeleton organization
TraesCS5B02G491800	Actin depolymerization factor-like protein	147	6.3E-104	88.78	0.86	-0.12	0.73	-2.31	1.92E-05	0.00021	Cytoskeleton organization
TraesCS5D02G492300	Actin depolymerization factor-like protein	147	6.3E-105	87.63	0.55	0.09	0.38	-3.25	2.08E-11	5.07E-10	Cytoskeleton organization
TraesCS1B02G069300	Protein unc-13 homolog	1107	0	93.26	9.87	9.73	10.07	1.73	1.97E-53	5.97E-51	Cell wall organization
TraesCS6D02G048900	Melibiose family protein	637	0	80.94	-2.04	-3.80	-2.48	-0.04	0.000177	0.001532	Cell wall organization
TraesCS1B02G084600	Hydroxyproline O-galactosyltransferase GALT3	591	0	83.91	3.76	2.71	2.78	0.79	5.51E-16	1.89E-14	Cell wall organization
TraesCS1D02G019000	Tricin synthase 1	248	1.8E-180	79.05	-1.48	0.37	-2.29	-0.17	6.39E-09	1.18E-07	Cell wall organization
TraesCS5D02G488900	Caffeic acid O-methyltransferase	353	0	86.01	-1.86	-2.56	-4.53	0.63	7.23E-20	3.17E-18	Cell wall organization

TraesCS1B02G098800	Acyl transferase 4	435	0	80.27	8.49	2.00	8.69	2.57	4.28E-31	3.63E-29	Cell wall organization
TraesCS3D02G116600	Alkane hydroxylase MAH1-like	517	0	88.56	0.02	0.08	-2.60	-2.99	0.001075	0.00741	Cell wall organization
TraesCS5D02G127300	Aldehyde dehydrogenase family 3 member H1-like	479	0	86.99	0.49	-0.29	-2.17	-1.78	2.63E-10	5.72E-09	Cell wall organization
TraesCS2A02G045800	GDSL esterase/lipase LTL1	369	0	90.05	9.20	1.62	8.58	8.50	3.69E-36	4.22E-34	Cell wall organization

3 Bold numbers indicate more than two-fold changes in expression.